The restoration of vascular function in murine vessels, ex vivo, using Ceria nanoparticles

Manchester Metropolitan University

MSc (By Research)

A thesis submitted in fulfilment of the requirements of the Manchester Metropolitan University for the degree of Master of Science (By Research)

Emily Si Lyn Tye

School of Healthcare Science
Faculty of Science and Engineering
Manchester Metropolitan University

ABSTRACT

Nanoparticles show an exciting opportunity within the medical field, such as in diagnostics or therapeutics, due to their capacity to be surface modified and loaded with dyes and drugs. Current clinical applications of nanoparticles include localisation in tumour cells for cancer therapy, delivery of nucleic acids and viral therapies such as HIV vaccination. An exciting area of nanomedicine is using nanotechnology to target inflammatory and chronic diseases that involve the generation of reactive oxygen species (ROS). Cerium provides excellent anti-ROS properties and its effect as a nanoparticle needs to be established.

The clinical application of nanoparticles often requires an entry point, one of which is intravenously done. Once injected into the bloodstream, the endothelial cells that line the blood vessel are one of the first sites of exposure, and because endothelial cells are important modulators of vascular function, the influence of silica and ceria-coated silica nanoparticle uptake on vasodilation and cerium's anti-ROS properties effect on vasodilation, remains unclear.The aim of the present study was to investigate the influence of silica and ceria-coated silica nanoparticles on vascular function of mouse aortic vessels, *ex vivo*.

Silica, ceria and ceria-coated silica nanoparticles were successfully synthesised and their physicochemical characterisation determined. Their effect on constrictor, and both endothelial dependent and independent dilator responses were assessed, using the organ bath technique and evaluation of uptake was also conducted using TEM.

The present study demonstrates two important findings. Firstly, that ceria-coated silica nanoparticles have an improved endothelial-dependent dilatory effect on young mouse aorta, whereas silica nanoparticles alone (C3) showed no detrimental effect on both

endothelial-dependent and -independent dilation. Secondly, that ceria-coated silica nanoparticles did not improve dilation in aged aortic vessels, and silica nanoparticles (C3) did not show to have a detrimental effect on dilation, since the dilator component in aged vessels was found to be similar to that in young vessels.

Contents

List of Figures

List of Tables

1. Introduction

1.1 Structure and Function of the Vasculature

Blood vessels are made up of three layers: tunica intima, tunica media and tunica adventitia.The tunica intima comprises of the endothelial basement membrane and the endothelial cells that lie on it. The tunica media comprises of smooth muscle cells that allow for constriction of the vessel and the tunica adventitia comprises of connective tissue. These layers can be seen in Figure 1.

Although the smooth muscle cells are responsible for the constriction of the vessel, endothelial cells themselves can also modulate vessel diameter by releasing a variety of mediators. Of those mediators, nitric oxide (NO), prostacyclin, and endothelial-dependent hyperpolarising factors (EDHFs). Some mediators can induce constriction of the vessel, such as endothelin. These mediators are highly regulated to ensure adequate blood flow and perfusion in the body. As the body ages, there can be an imbalance of these mediators being released which leads to 'endothelial dysfunction'. This imbalance can also be seen in the early stages of cardiovascular disease.

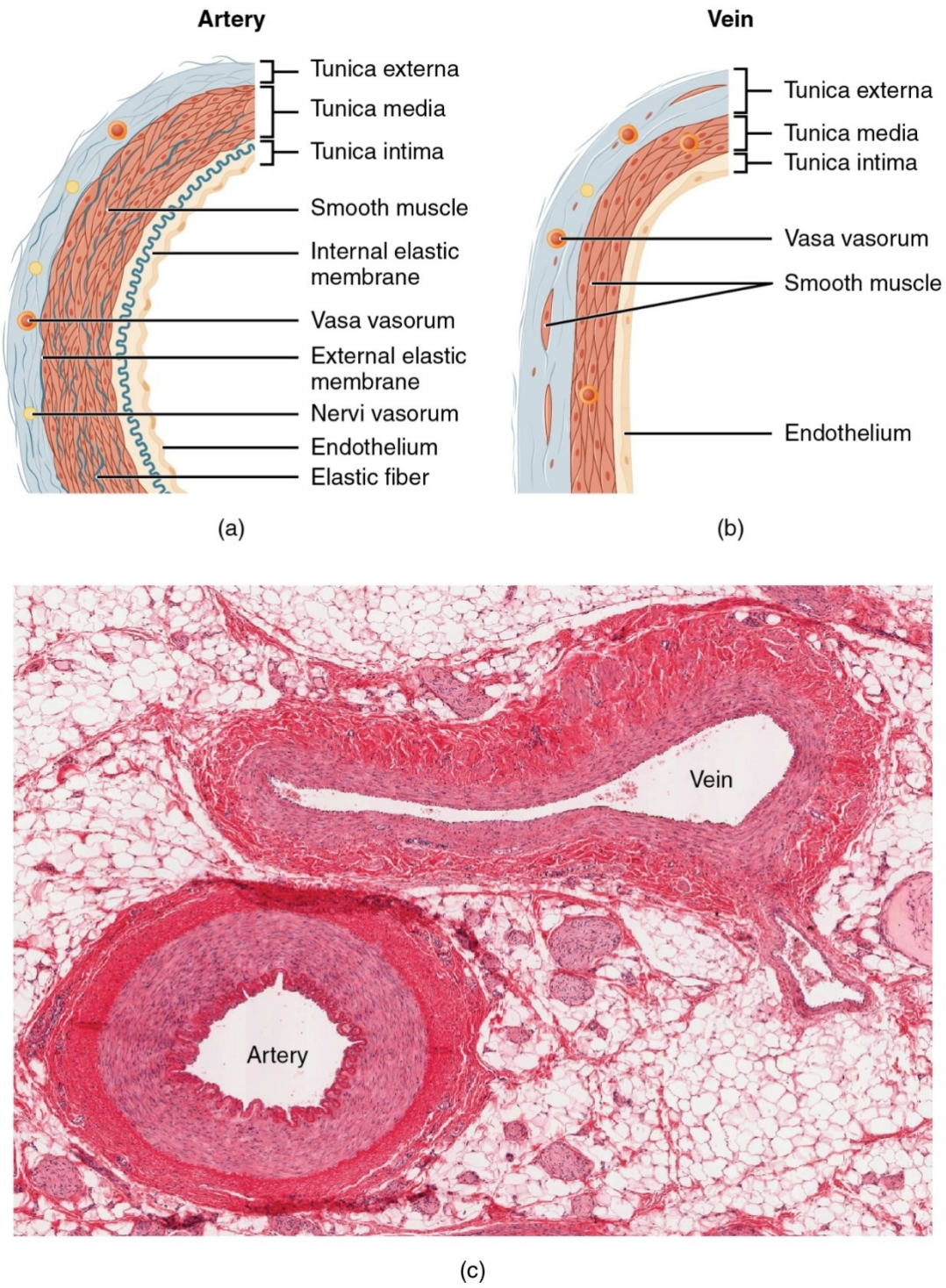

Figure 1 A diagram depicting the structure of (a) an artery (b) a vein and (c) a sample from human tissue showing a cross section of an artery and a vein. Image taken from (OpenStax College 2014)

1.2Mitochondrial/Free-Radical Theory of Ageing

Due to medical advancements, improved sanitation and better personal care, there is an ever-increasing ageing population. Whilst ageing might not necessarily be synonymous with disease, it is thought to be a risk factor or associated indirectly to risk factors that contribute to disease (Lakatta and Levy 2003).

There are currently a number of theories that try to explain why the ageing process occurs and what mechanisms lead to it, including the mitochondrial/free-radical theory of ageing. During normal respiration in the cell, the mitochondria is the location for the electron transport chain in which oxygen is converted into water which produces energy(Judge, Jang et al. 2005). This process, however, is not one hundred percent efficient as a small percent of the oxygen ends up being converted to reactive oxygen species (ROS) which are unstable and have unpaired electrons. These include peroxides (H_2O_2), superoxide (O^{2-}), hydroxyl radical (OH^-), and singlet oxygen (O_2). These then are able to attach onto lipids, proteins and nucleic acids and alter their structure or composition. They also affect the mitochondrial DNA (mtDNA) that produce polypeptides which enable the electron transport chain to work efficiently. As these polypeptides get damaged, it spawns a negative cycle of more ROS being produced which in turn damage the polypeptides further. This leads to a decline in energy available and increases the amount of ROS produced. This decline in energy and the increased in ROS production is what is considered the cause of ageing and ageing-related diseases(Bratic and Larsson 2013).

1.2 ROS and Cardiovascular Disease

Ageing has been considered a risk factor for cardiovascular diseases amongst others, such as sedentary lifestyle, diet, and genetics(Spiteller 2001).Cardiovascular diseases are responsible for the most deaths worldwide and involve changes in the vasculature which

lead to a decline in function. These changes include calcification, atherosclerosis and, endothelial dysfunction(Kovacic, Moreno et al. 2011). Nitric oxide (NO), a potent vasodilator, is involved in the regulation of vascular tone and is released continuously by endothelial cells *via* the conversion of arginine to citrulline(Tousoulis 2012). ROS leads to a reduction in NO levels which ultimately lead to a reduction in endothelial cell mediated vasodilation(van der Loo, Labugger et al. 2000) and leads to endothelium dysfunction. ROS also causes upregulation of the protein complex, nuclear factor kappaB (NF-κB) causing it to shift the vasculature to a more pro-thrombotic state (Donato, et al. 2007; Kollander, et al. 2010) which can contribute to risk of cardiovascular disease. Currently, most of the treatment options for ROS are nutritional supplementation of known antioxidants such as beta-carotene and vitamin E which are thought to reduce ROS levels. They do not reflect the same result in clinical trials (Vivekananthan, Penn et al. 2003) and therefore there is a need for better substances with antioxidant properties.

Because ROS contain unpaired electrons, which make them unstable and highly reactive, current treatment revolves around antioxidants, and other substances, and their ability to neutralise and counteract against these unpaired electrons, effectively removing their ability to cause damage and bind to other molecules as efficiently.

1.3 ROS Treatments: Nutritional Supplementation

Nutritional supplementation of known antioxidants have been investigated on their effect on ROS levels. Vitamin E has been shown to have antioxidant like properties due to their scavenging ability of singlet oxygen (Lee, Koo et al. 2004) although it is mainly involved in protecting against lipid peroxidation (Pryor 2000). It works along with ascorbic acid (vitamin C) to maintain recyclability (Kojo 2004). It has been shown to be protective against heart disease and cancer (Meydani 2000). A study by(Yatin, Varadarajan et al. 2000) found that when rats were supplemented with vitamin E, it prevented the increase in ROS which was induced chemically. Vitamin C has been found to be an important antioxidant, with its ability to donate electrons and stabilising ROS. Supplementation of vitamin C has been shown to prevent heart disease, various cancers and protect against oxidative stress induced by smoking (Lee, Koo et al. 2004). Carotenoids have been found to have antioxidant properties as they donate electrons to ROS, however some of the trials conducted have shown it to be ineffective and may even detrimental to lowering ROS. Other suggestions have included, plant sterols (De Jong, Plat et al. 2007), however, they did not affect oxidative stress; grape polyphenols including resveratrol, flavans, and anthocyanins were found to decrease whole-body levels of oxidative stress in pre- and post-menopausal women (Zern, Wood et al. 2005); green tea polyphenols were found to protect human skin that was subjected to ultraviolet radiation-induced oxidative stress (Katiyar, Perez et al. 2000); alpha-Lipoic acid was found to protect against insulin resistance that was induced by oxidative stress (Maddux, See et al. 2001). There have been numerous human clinical trials investigating various antioxidants, such as vitamin E and beta-carotene, and their effectiveness in treating cardiovascular disease, however, these trials have largely been unsuccessful (Vivekananthan, Penn et al. 2003) and more research is needed to evaluate other antioxidants for treatment of oxidative stress.

1.3.1 ROS Treatments: Pharmaceutical Treatment

Pharmaceutical treatments have also surfaced that have been investigated for their effect on ROS levels. It is thought that the cardiovascular drugs prescribed owe their effectiveness to their indirect antioxidant properties (Weseler and Bast 2010) for example angiotensin-converting enzyme (ACE) inhibitors have been shown to have antioxidant activity (Bartosz, Kedziora et al. 1997). A study by(Pashkow, Watumull et al. 2008) proposed a novel molecule for treatment of oxidative stress, named astaxanthin, which was found to have antioxidant properties and looked promising as a candidate for cardiovascular oxidative stress. Other newly designed pharmaceutical aids that have antioxidant properties have been produced that mimic the structure of naturally occurring antioxidants (Weseler and Bast 2010).

1.4. Current clinical applications of nanoparticles

Nanoparticles have many potential benefits to medicine and current clinical applications include, diagnosis and treatment of cancer using quantum dots or nanoparticles made from dyes (Radenkovic, et al. 2016; Patra, 2016). Another area using nanoparticles is for the delivery of nucleic acids for treatment of genetic or regenerative diseases (Cheng and Lee. 2016; Chen, et al. 2016). Nanoparticles can also be used for the vaccination of certain viruses, including HIV (Glass, et al. 2016).

1.5. Nanoparticles and their potential role in ROS treatment

Because ROS is implicated in many diseases and in ageing, there is a need for an effective treatment option that is able to neutralise ROS whilst maintaining minimal side effects. One of these options involves the use of nanoparticles which have antioxidant capabilities.

Nanoparticles, as defined by the British Standards Institution, are particles with two or more dimensions in the nanoscale, between 1 and 100nm (BSI 2011). At this scale, nanoparticles exhibit different properties compared to their corresponding bulk materials. These properties include having a high surface area to volume ratio, unique quantum properties, as well as the ability to be modified with other molecules and materials. It is because of these properties that they have been considered in many different fields including in medicine. Nanoparticles have been considered for biomedical applications due to their small size, so that they are able to be taken up by cells. Nanoparticles have the ability to be modified, which can be used in targeted drug delivery. By targeting certain marker molecules, it can also be used to help identify levels of pathogens, or levels of genes, protein or metabolites in a sample (Baptista, Doria et al. 2011). Nanoparticles have also been considered for therapeutics, especially for cancer therapy (Alexis, Pridgen et al. 2009), and wound healing

(Krausz, Adler et al. 2015). There are some considerations for the material used to make the nanoparticles. It can be that the material itself possesses properties that can be biologically relevant, or that the material can be used to made to be mesoporous and allow for encapsulation of drugs or other molecules.

1.6Nanoparticles and their effect on vasculature

Nanoparticles used in clinical applications are often administered intravenously and therefore the effects on the vasculature need to be established so that the endothelial cell function is not compromised. Studies have looked at various types of nanoparticles and their effect on vascular function. A study by Gojova, et al. (2007) looked at different types of nanoparticles (iron oxide, yttrium oxide, and zinc oxide) and found that yttrium oxide and zinc oxide nanoparticles elicited an inflammatory response in human aortic endothelial cells following short-term exposure. A research report written for the Health Effects Institute (Boston, Massachusetts, USA) by Kennedy, et al. (2009) reviewed the effects of various nanoparticles (cerium, iron, zinc, and yttrium oxide) on human aortic endothelial cells, looking at markers of inflammation and generation of ROS and oxidative stress. They found that the zinc oxide nanoparticles induced inflammation and oxidative stress, whereas yttrium oxide increased in some of the markers, and iron oxide and cerium oxide did not induce inflammation or oxidative stress. These differences can be pinned down to the physical and chemical properties of the nanoparticles. A study by Farooq, et al. (2014) found that silica nanoparticles, after incubation, attenuated endothelial dependent vasodilator responses in rats and subsequent incubation in cerium oxide nanoparticles restored this attenuation.

1.7Ceria Nanoparticles and their role in ROS treatment

1.7.1. Antioxidant property of cerium

Cerium is the most abundant metal in the rare metal group named lanthanides(Hedrick 2004). Cerium oxide have the ability to switch between its two oxidation states, 3+ and 4+, which gives it redox properties. Although the bulk material has these properties that are attractive to be used as an antioxidant, it is biologically more applicable to produce cerium oxide nanoparticles instead.

1.7.2. Ceria nanoparticles and their effects on vascular and physiological function

Ceria nanoparticles mimic superoxide dismutase and are a possible therapeutic option for ROS-related conditions. A recent study (Farooq, Mohamed et al. 2014)investigated vascular dilatory responses after incubation with nanoparticles and found that the attenuated dilation after treatment with silica nanoparticles, was partially restored after coating nanoparticles in ceria. From this, it was suggested that ceria nanoparticles could be used as a therapeutic option for the treatment of impaired vascular responses.

Ceria nanoparticles have been found to have beneficial effects on physiological systems.A study (Kolattukudy, Quach et al. 1998) injected ceria nanoparticles into transgenic mice which expressed the monocyte chemo-attractant protein-1 (MCP-1) which, in control mice, induced myocardial inflammation and caused ischemic cardiomyopathy. It was found that mice that were injected with ceria nanoparticles did not exhibit as many clinical symptoms or were much milder than the controls. A study (Rzigalinski, Meehan et al. 2006) used *Drosophilia* as an animal model and found that consumption of ceria nanoparticles lead to an increased lifespan when compared to the controls, which was incidently similar to the

findings when *Drosophilia* is genetically altered to over-express SOD, it is found to increase lifespan by 30%. Ceria nanoparticles have been found to be biocompatible and not exert any toxic effects. Histology alterations were not seen, 30 days after nanoparticles were administered (Hirst, Karakoti et al. 2009) and there was no increased number of deaths after nanoparticle administration compared to controls, within 9 weeks (Xia, Kovochich et al. 2008). Ceria nanoparticles have been considered for use as a drug delivery system. The nanoparticles were responsive to increased reactive oxygen species and was shown to have a significant effect on drug loading for treating cancer (Muhammad, Wang et al. 2014). Ceria nanoparticles have been found to enhance radiotherapy treatment in cancer cells, by causing arresting cell cycle at the G2/M stage, inducing autophagy and increasing rate of cell death, when compared to radiation alone. It was interesting to note that ceria nanoparticles, alone, were not toxic to the cancer cells. These findings have clinical impact as ceria nanoparticles can increase sensitivity of cancer cells to radiation and may be used in conjunction with radiotherapy (Chen, Zhang et al. 2015).

1.7.4. Ceria nanoparticles and their effects on cellular function

Ceria (CeO_2) nanoparticles have been of particular interest in regards to vascular disorders due to their antioxidant properties (Heckert, Karakoti et al. 2008). The free radical scavenging ability of ceria may be due to the ratio of Ce^{3+}/Ce^{4+} ions rather than the oxygen vacancies present. A high Ce^{3+} concentration is also favoured due to its enhanced superoxide dismutase (SOD) mimetic activity when compared to Ce^{4+}(Karakoti et al. 2008). Whereas a lot of the literature supports the fact that a high Ce^{3+}/Ce^{4+} ratio is necessary for its superoxide dismutase scavenging effects, a recent publication has found that there is an inhibition of these effects when ceria nanoparticles are in the presence of phosphate ions, as they interfere with the Ce^{3+} sites of the nanoparticles (McCormack, Mendez et al. 2014). Ceria nanoparticles have also been demonstrated to enhance cyto-protection of beta cells

from exposure to superoxide (Weaver and Stabler 2015). However, the group found that uptake of the ceria nanoparticles did cause cytotoxicity. This lead to them to produce a hydrogel containing ceria nanoparticles which provided the cyto-protection without the uptake and cytotoxicity, even when high concentrations of ceria nanoparticles were used. Ceria nanoparticles have been investigated in the treatment of age-related male infertility. Using rats as an animal model, ceria nanoparticles have been found to reduce ROS, increase catalase and SOD activity as well as improve sperm count and other parameters (Kobyliak, Falalyeyeva et al. 2015). Ceria nanoparticles have been found to exhibit antioxidant properties that provide protection in neurons from rat spinal cords whilst being biologically compatible as well as regenerative (Das, Patil et al. 2007). Ceria nanoparticles were found to be deposited in tissues in *in vivo* studies and reduced oxidative stress to the same level as a common therapeutic used to lower oxidative stress (Hirst, Karakoti et al. 2013). A study (Kim, Kim et al. 2012) found that ceria nanoparticles were able to reduce ischemic brain damage as well as targeting damaged areas specifically. A study (Niu, Azfer et al. 2007) found that ceria nanoparticles prevented the progression of cardiac dysfunction by lowering oxidative stress and inflammation in mice. Ceria nanoparticles were also been investigated for the treatment of neurodegenerative diseases such as Parkinson's disease. Ceria nanoparticles were able to reduce oxidative stress in PC12 cells that had been induced using manganese chloride, instead of the more commonly used hydrogen peroxide. Ceria nanoparticles were found to have a protective role and have potential for therapeutic use in Parkinson-like diseases (Pinna, Malfatti et al. 2015).

In order to functionalise ceria nanoparticles, anchors may be needed to allow for molecules to bind to them. (Yang, Luo et al. 2014) studied the effectiveness of alendronate as an anchor, as it was found to have a high binding affinity to ceria nanoparticles and did not hinder ceria's activity. It was also found to improve stability and reduce cytotoxicity. In a recent study, ceria nanoparticles have been coated with polyethylene glycol (PEG), using

alendronate as an anchor (Li, Yang et al. 2015). These nanoparticles were found to be more stable than naked ceria nanoparticles and were found to be more effective at protecting human hepatocytes from damage induced by gamma-radiation. The group also found that the PEGylated ceria nanoparticles contributed to an increase in SOD expression, which aids in the protection against ROS. Ceria nanoparticles were also investigated in its effect on the nuclear factor erythroid-2 (Nrf-2)/hemoxygenase-1 (HO-1) pathway which is implicated when there is oxidative stress from D-galactoseamine and lipopolysaccharide-induced hepatotoxicity. The ceria nanoparticles have been found to decrease translocation of Nrf-2, which brings about an antioxidative effect demonstrated by the increased levels of SOD and catalase (Hashem, Rashd et al. 2015). Dextran is another biocompatible polymer that can be used to coat ceria nanoparticles without inhibiting its antioxidant effect. They have been found to be cytotoxic to osteosarcoma cells, although a high concentration was needed, 250μg/mL, in order for the bone cancer cells to be killed. It is suggested that the dextran coating may play a role in ceria's antioxidant/oxidant properties and its oxidant properties may be triggered due to the tumour microenvironment allowing for tumour selectivity (Yazici, Alpaslan et al. 2015).

Ceria nanoparticles have been investigated in cellular studies. Ceria nanoparticles have been found to prevent oxidative stress in human umbilical vein endothelial cells by counteracting ROS using hydrogen peroxide. There was also a reduction in apoptosis and necrosis seen after uptake of nanoparticles. The mechanisms of uptake were investigated and it was found that the nanoparticles were taken up by endocytosis mediated by caveolae and clatharin, and were found throughout the cytoplasm (Chen, Hou et al. 2013). Ceria nanoparticles and mechanisms of exocytosis were also investigated in human microvascular endothelial cells and it was found that after uptake, nanoparticles that accumulate in the vesicles of the cell are emptied and it is thought that this process would

protect endothelial cells from accumulation of nanoparticles and its possible adverse effects (Strobel, Oehring et al. 2015).

1.7.6. Conclusion

As ceria nanoparticles have been investigated for its antioxidant ability, there is a question as to whether ceria nanoparticles can improve vascular function that may have been compromised during ageing, without any other symptoms of disease.

1.8 Silica nanoparticles and their effect on vasculature

Silica nanoparticles have also been investigated for many uses within medicine. The production of mesoporous (containing many pores) silica nanoparticles allows it to hold and deliver drugs as well as dyes for diagnostics (Tang, et al. 2012).

With so many studies looking at the biomedical applications of these nanoparticles, more work is needed to assess their effect on the physiological system, including the vascular system. A study by Liu, et al. (2010) found that expose to silica nanoparticles in human umbilical cord vein endothelial cells resulted in the production of intracellular ROS which lead to endothelial dysfunction via oxidative stress. It has also been demonstrated, in previous work done by the group, that silica nanoparticlescan influence dilator responses in aortic vessels, depending on size, charge and dye encapsulation (Akbar et al, 2011; Farooq et al, 2013). A reduced dilator response from incubation with silica nanoparticles could then be partially restored when there was incubation with ceria-coated silica nanoparticles (Farooq et al, 2014). Hence, responses to ceria, silica, and ceria coated silica in aortic vessels from young and aged mice, will be examined in the present study.

1.9Methodologies for fabricating silica and ceria nanoparticles

For silica nanoparticles, Stöber (Stöber, Fink et al. 1968) produced a method that was able to build up, through nucleation and other growth processes, a monodispersed colloid solution of spherical nanoparticles.

For cerium oxide (ceria), there have been many different protocols used to produce them and no gold standard protocol has been found and adopted. So far, the different methods of synthesis include: hydrothermal (Masui, Hirai et al. 2002), precipitation (Chen and Chang 2005), using supercritical fluid technology (Byrappa, Ohara et al. 2008), reverse micellar (Sathyamurthy, Leonard et al. 2005), and flame electrospray pyrolysis (Oh and Kim 2007). Due to the aggregated nature of ceria nanoparticles, coatings have been considered to result in a colloidal, well-dispersed solution. Coatings can electrostatically repel the nanoparticles (Mandzy, Grulke et al. 2005), or can be polymers (Corbierre, Cameron et al. 2001) to make sure the ceria doesn't aggregate and get into contact with each other. Biocompatibility is another issue when thinking about adding extra materials onto the nanoparticle. If the coatings interfere with biological responses, it would be undesirable to continue working with them in the areas of nanomedicine.

1.10Nanoparticle Characterisation

There are a range of techniques that are adopted to look at the properties of nanoparticles and determine their size, dispersion, aggregation and charge, as follows:

1.10.1 Scanning electron microscopy

This technique analyses size and morphology of nanoparticles by coating the sample with a thin layer of gold, which is then subjected to a beam of electrons that are scanned across the sample. When the electrons hit the sample, secondary electrons and scattered electrons are detected and are used to form an image. In Figure 2, the structure of the microscope can be seen.

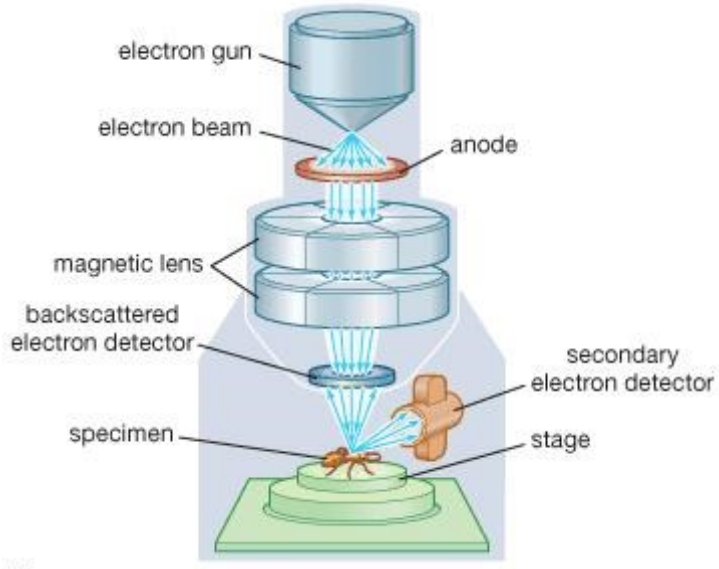

Figure 2 Image depicting the structure of a scanning electron microscope (taken from (Bradbury 2008))

1.10.2 Transmission electron microscopy

A transmission electron microscope works similarly to a light microscope except it uses electrons as the source instead of light. These electrons are beamed onto the sample and are scattered based in density of the sample. Those electrons that do not scatter end up passing through the sample and onto a fluorescent screen which then gives an image of the sample with different parts of the sample showing varying degrees of darkness depending on their density. This technique is used to analyse size and morphology of the nanoparticles. The structure of a transmission electron microscope can be seen in Figure 3.

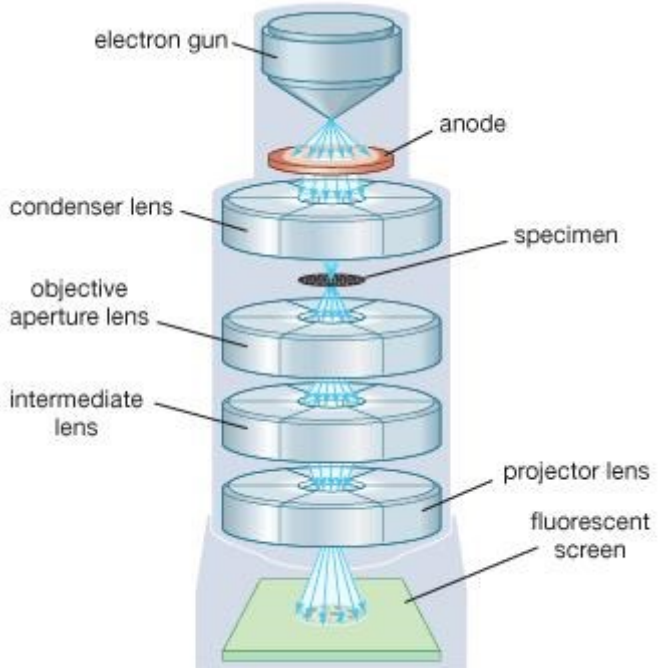

Figure 3 An image depicting the structure of a transmission electron microscope (taken from (Ford 2008))

1.10.3 Dynamic light scattering

This technique is also known as photon correlation spectroscopy and is based on the principle of Brownian motion, that is, the random movement of particles within a solution. The smaller the particle is, the faster the velocity in which they travelled. When using dynamic light scattering, a laser beam is focused through the sample. The particles within the sample diffract the laser beam and cause fluctuations in the scattering intensity, which correlates to the hydrodynamic diameter of the particle. The hydrodynamic diameter includes the diameter of the particle plus an electric dipole layer that forms from the solvent. This technique is used to analyse hydrodynamic diameter of nanoparticles in different solutions.

1.10.4 Ultraviolet-visible spectroscopy

This technique involves passing a spectrum of light, ranging from ultraviolet to visible, through a sample and measuring the absorbance of the light through the spectrum. The peaks of absorption can reveal information about the sample. In the case of cerium, the different absorption peaks allow the differentiation between cerium with a 3+ oxidation state, and cerium with a 4+ oxidation state. A peak at around 413nm indicates the presence of cerium 3+, and a peak at around 310nm indicates the presence of cerium 4+.

1.10.5 Zeta potential analysis

This technique investigates the surface charge of nanoparticles when in solution. The particles, as mentioned before, have an electrical dipole layer caused by ions in the solution being attracted to the slight surface charge of the nanoparticle. The electrical potential on the boundary of this ion attraction, known as the electrical double layer, is known as the zeta potential. Zeta potential values of less than -25mV or greater than +25mV are considered to have high stability. Nanoparticles with zeta potential values within that range will be subjected to Van der Waals attraction with each other and cause aggregation over time (NanoComposix 2012).

1.11 Aims and Objectives

The overall aim was to investigate the influence of silica, ceria, and ceria-coated silica nanoparticles on vascular function of mouse aortic vessels, ex vivo.

The specific objectives were as follows:

1. To fabricate and characterise silica, ceria, and ceria coated silica nanoparticles, using physicochemical characterisation techniques
2. To determine the dilator response of aortic vessels in young and aged mice, *ex vivo*, using the organ bath technique
3. To elucidate the influence of silica, and ceria coated silica nanoparticles on the functional (i.e. contractile and dilator) responses of isolated blood vessels from young and aged mice, *ex vivo*, using the organ bath technique.

The Null Hypothesis is:

1. There is no difference in the dilator response of aortic vessels between young and aged mice.
2. Ceria-coated silica nanoparticles will have no influence on the dilator function of aged mouse aortic vessels.

The Alternative hypothesis is:

1. The dilator response of aortic vessels in aged mice is significantly reduced, in comparison to young mice
2. Ceria-coated silica nanoparticles are able to restore dilator function in aortic vessels from aged mice.

2. Objective 1: Fabrication and Characterisation of Nanoparticles

2.1. Preparation of Ceria and steric stabilised ceria Nanoparticles

In this present study, there were many methods that were used to make ceria nanoparticles and there was a need to establish the best methodology to be used. Ceria nanoparticles (<25nm in size) were also purchased from Sigma Aldrich, UK. Table 1 below, provides an overview of the range of methods used.

Table 1 Overview of methodologies used to produce ceria and steric stabilised ceria nanoparticles

Ceria nanoparticle batch	Reference	Overview of methodology	Modifications
CeA	(Farooq, Mohamed et al. 2014)	Cerium salt was dissolved in ethanol and was stirred into a sodium hydroxide solution (sodium hydroxide and ethanol). This was stirred and afterwards, hydrogen peroxide was added to form the precursor solution. Nitric acid and sodium hydroxide was added to the precursor and the product was centrifuged.	N/A

CeB	(Chen and Chang 2005)	Cerium salt solution was heated with ammonium hydroxide solution. This was stirred and centrifuged.	PVP coating added post-production
Sigma Ceria	Sigma Aldrich, UK	No methodology provided with commercially bought ceria nanoparticles	PVP coating added post-production
CeE	(He, Wu et al. 2012)	Cerium salt, urea and PVP were dissolved into water. This was heated and ammonium hydroxide was added. This was stirred and centrifuged.	PVP coating added during production
CeF	(Izu, Uchida et al. 2011)	PVP and cerium salt were dissolved into ethylene glycol. This was heated and stirred. The product was centrifuged.	PVP coating added during production
CeG	Adapted from (He, Wu et al. 2012)	Cerium salt, urea and dextran were dissolved into water. This was heated and ammonium hydroxide was added. This was stirred and centrifuged.	Dextran coating added during production

CeA Method

The method was taken from Farooq et al. (Farooq, Mohamed et al. 2014). Materials include: cerium nitrate hexahydrate (Sigma Aldrich, UK), industrial methylated spirit, sodium hydroxide, hydrogen peroxide (30%), distilled water and nitric acid (70%).

One gram of cerium nitrate hexahydrate was stirred into 15.78 mL of industrial methylated spirit, and left stirring vigorously at 50C in a paraffin oil bath. In a separate vial, 1g of sodium hydroxide was stirred into 15.78 grams of industrial methylated spirit. The sodium hydroxide solution was added dropwise into the cerium nitrate solution and was stirred vigorously for twenty-four hours at 50C in a paraffin oil bath. Once cooled, 0.05mL of hydrogen peroxide was added and stirred for one hour. The precipitate formed was then centrifuged at 6000rpm for 20 minutes and the pellet was re-dispersed into 20mL distilled water. The solution's pH was adjusted to pH 0.14 using 2mL of nitric acid. The solution was heated to 40C for 2 hours and left to cool afterwards at room temperature. This was the precursor solution.

3mL of this solution was then dispersed into 30mL of distilled water whilst stirring. The mixture was then stirred vigorously for 30 minutes. The pH was adjusted to 9.1 using 5mL of sodium hydroxide solution (1M), which was added dropwise into the solution. It was then stirred for 3 hours and 35 minutes at 60C in a paraffin oil bath. The product was then centrifuged for 30 minutes and cleaned with water several times.

CeB Method

The method was taken from Chen and Chang (Chen and Chang 2005). Materials include: 0.2M cerium nitrate hexahydrate (Sigma Aldrich, UK) and 3M ammonium hydroxide.

Fifty millilitres of cerium nitrate solution was heated to 70C in a paraffin oil bath and stirred vigorously. 25mL of the ammonium hydroxide solution was added to the cerium nitrate solution. This solution is left at 70C for 20 hours. The solution is then centrifuged at 6000rpm for 20 minutes and cleaned with water several times.

Commercially bought Ceria (Sigma Aldrich, UK)

The method of production for these nanoparticles were not given. This product was purchased from Sigma Aldrich UK and the product code was '*544841ALDRICH*'.

2.2 Preparation of steric-stabilised Ceria Nanoparticles

With aggregation being apparent in the ceria nanoparticles, it was decided that steric stabilisation was to be used in order to produce ceria nanoparticles without the aggregation and help form more individual nanoparticles. Two types of polymers were used to sterically stablise the nanoparticles, polyvinyl pyrrolidone (PVP) and dextran, which is polymerised glucose.

Adding PVP onto nanoparticles

CeB2PVP Method

This method was adapted from Graf, et al. (Graf, Vossen et al. 2003). Materials included: ceria nanoparticles made from CeB method, PVP (molecular weight of 10,000 Daltons) and distilled water.

6.9uL of CeB nanoparticles were resuspended in 40mL of distilled water to get a concentration of $1.44x10^{14}$ nanoparticles per mL. This solution was sonicated for 15 minutes and then placed in a round bottomed flask and stirred using a magnetic flea stirrer. PVP solution was produced by dissolving 0.06g in 2.6mL of distilled water. This PVP solution was added into the ceria nanoparticle solution and was stirred for 24 hours.

CeSigPVP Method

This method was adapted from Graf, et al. (Graf, Vossen et al. 2003). Materials included: ceria nanoparticles (purchased from Sigma Aldrich, UK), PVP (molecular weight of 10,000 Daltons) and distilled water.

0.01g of ceria nanoparticles were suspended in 25mL of distilled water to get a concentration of $1.72x10^{14}$ nanoparticles per mL. This solution was sonicated for 15 minutes and then placed in a round bottomed flask and stirred using a magnetic flea stirrer. PVP solution was produced by dissolving 0.33g in 4mL of distilled water. This PVP solution was added into the ceria nanoparticle solution and was stirred for 24 hours.

CeE Method

The method was taken from He, et al. (He, Wu et al. 2012). Materials include: distilled water, cerium nitrate hexahydrate, urea, ammonium hydroxide (70%), and PVP (molecular weight of 10,000 Daltons)

The cerium nitrate hexahydrate, urea and PVP were dissolved in the water. This was then heated to 70C in a paraffin oil bath for 1 hour, and stirred vigorously. Ammonium hydroxide was then added dropwise. Once a pale yellow precipitate had formed, the reaction was stopped and cooled to room temperature. It was then centrifuged at 6000rpm for 20 minutes and cleaned several times with water.

CeF Method

The method was taken from Izu, et al. (Izu, Uchida et al. 2011). Materials included: ethylene glycol, PVP (molecular weight of 10,000 Daltons) and cerium nitrate hexahydrate.

PVP (3.15g) and 7.82g of cerium nitrate hexahydrate were added to 30cm^3 of ethylene glycol and stirred until dissolved. The solution was then transferred to a silicone oil bath at 140C for 2 hours. It was then cooled to room temperature.

Adding dextran onto nanoparticles

CeG Method

The method was adapted from He, et al. (He, Wu et al. 2012), but used dextran to coat the nanoparticles instead of the PVP. Materials included: cerium hexahydrate, urea, distilled water, ammonium hydroxide and dextran (molecular weight of 500,000 Daltons).

The cerium nitrate hexahydrate, urea and dextran were dissolved in the water. This was then heated to 70C in a paraffin oil bath for 1 hour, and stirred vigorously. Ammonium hydroxide was then added dropwise. Once a pale yellow precipitate had formed, the reaction was stopped and cooled to room temperature. It was then centrifuged at 6000rpm for 20 minutes and cleaned several times with water.

2.3Preparation of silica nanoparticles

For the silica nanoparticles, there were two different types of methodologies used. SilA and SilB used the same method, but altered concentrations, to produce different sized nanoparticles, and SilC was done using a different method. Silica nanoparticles (A3) were also kindly provided by Ali Shukur. AN overview of the methods can be seen in Table 2.

Table 2Overview of the methodologies used to produce silica nanoparticles

Silica nanoparticle batch	Reference	Overview of methodology	Modifications
SilA	(Bagwe, Yang et al. 2004)	Triton X-100, cyclohexane, hexanol and water were stirred. Rhodamine dye was added, followed by TEOS and ammonium hydroxide. Product was retrieved by rotary evaporation and centrifuged.	Rhodamine dye encapsulated
SilB	(Bagwe, Yang et al. 2004)	Details are the same as above using a different ratio of the materials.	Rhodamine dye encapsulated
SilC	(Farooq, Mohamed et al. 2014)	Ammonium hydroxide was added to ethanol and water. This solution was heated, and TEOS was added to it. This was then stirred and centrifuged.	Ceria coating post-production
A3	(Stöber, Fink et al. 1968, Ibrahim, Zikry et al. 2010)	Ammonium hydroxide, ethanol, TEOS and double distilled water was stirred. Rhodmaine dye was added to this solution. This was then stirred and centrifuged.	Rhodamine dye encapsulated

SilA and SilB Method

This method was taken and modified from Bagwe, et al. (Bagwe, Yang et al. 2004). Materials included: rhodamine B isothiocyanate (RITC), (3-aminopropyl)triethoxysilane (APS), chloroform, Triton X-100, cyclohexane, hexanol, distilled water, tetraethyl orthosilicate (TEOS), and ammonium hydroxide. Quantities used for each chemical can be found in Table 3.

The rhodamine dye was produced by pipetting 0.02mL of APS and 0.2mL of chloroform in a small vial. Weigh out 0.02g of RITC and transfer into the vial. Place a magnetic flea stirrer into the vial and leave to stir overnight at room temperature.

Table 3 Quantities of materials needed to produce silica nanoparticles using reverse microemulsion

Sample Name	Rhodamine dye (µL)	Triton X-100 (mL)	Cyclohexane (mL)	Hexanol (mL)	Distilled Water (mL)	TEOS (mL)	Ammonium hydroxide (mL)
SilA	100	1.77	7.5	1.8	0.40	0.2	0.10
SilB	100	7.10	3.0	7.2	2.25	0.4	0.24

Using a glass Pasteur pipette take, Triton X-100, cyclohexane, hexanol and water were placed into a round bottomed flask and stirred for 15 minutes at room temperature using a magnetic flea stirrer. The rhodamine dye was slowly added in and the solution was stirred for an hour at room temperature. TEOS and ammonium hydroxide was added to the solution and it was stirred for 24 hours at room temperature.

Once the reaction had completed, products were recovered by rotary evaporation at 30C until there is little solvent left. The nanoparticles were isolated by acetone and centrifuged for 20 minutes at 6000rpm, and washed with ethanol and water several times.

SilC Method

The method was taken from Farooq, et al. (Farooq, Mohamed et al. 2014). Materials included: distilled water, ammonium hydroxide, industrial methylated spirit, TEOS.

Ammonium hydroxide (6.53mL) was added to a solution containing 88.3mL of ethanol and 1.91mL of water, which is heated in a silicone oil bath to 60C. Separately, a solution containing 2.27mL of TEOS and 2.23mL of ethanol was mixed. The TEOS solution was added drop-wise to the ammonium hydroxide solution and was stirred vigorously for 21 hours at 60C. Once cooled, it was centrifuged at 6000rpm for 30 minutes and washed with ethanol and water several times.

A3 Silica

These nanoparticles were kindly provided by Ali Shukur, who had produced them, using the methodology outlined in (Stöber, Fink et al. 1968, Ibrahim, Zikry et al. 2010) with modifications outlined below. Materials included: double distilled water, ethanol, ammonium hydroxide, TEOS, RITC, and APS.

Firstly, the rhodamine dye was produced by adding 40mg of RITC into 600µL of APS, and was stirred at room temperature using a magnetic flea stirrer. The reaction vessel was filled with nitrogen gas and mechanically stirred for 3 hours, in the absence of light.

In a separate vial, 4.89mL of ammonium hydroxide, 250mL of ethanol, 2.9775mL of double distilled water and 3.776g of TEOS solution were stirred using a magnetic flea stirrer for 15 minutes at room temperature. 50µL of the rhodamine dye was added, and this combined solution was stirred for 3 hours at room temperature.

The solution was centrifuged at 6000rpm for 20 minutes, and the supernatant was removed. Ethanol was added to the centrifuge tube and the precipitate was re-dispersed by vortex and ultrasonication. The solution was then re-centrifuged at 6000rpm for 20 minutes and the supernatant was discarded again. The precipitate was then re-dispersed in distilled water.

2.4 Preparation of Ceria-coated Silica Nanoparticles

The method was taken from Farooq, et al. (Farooq, Mohamed et al. 2014). Materials included: silica nanoparticles produced using SilC method, and ceria precursor from CeA.

0.1g of the silica nanoparticles were dispersed in 30mL of distilled water and 3mL of cerium precursor solution. It was stirred for 30 minutes and the pH was adjusted to 9 by adding ammonium hydroxide. It was then stirred for 4 hours at 60C, in a silicon oil bath. It was then centrifuged at 6000rpm for 30 minutes, and washed with water and ethanol several times.

2.5Size and morphology analysis of nanoparticles

The size and morphology of the nanoparticles was assessed using both scanning electron microscopy (SEM) and transmission electron microscopy (TEM). Dilute nanoparticle solution (10 µL) was dried onto a clean silicon surface and imaged by field emission gun (FEG) SEM (Carl Zeiss Supra 40VP

FEG, Carl Zeiss,WelwynGarden City, Hertfordshire,UK); or placed on a mesh copper grid and imaged using the Tecnai 12 Biotwin TEM at 80 kV, at the University of Manchester.

For SEM, the size of the nanoparticles were calculated using the SEM images (Figure 2), taking an average of 9 nanoparticle sizes. This sample size of 9 was chosen as it was the maximum amount of size measurements that can be taken electronically using the software provided. Manual measurements, although an option, would be less accurate.

2.6Physicochemical characterisation of nanoparticles

Physicochemical characterisation techniques include analysing hydrodynamic diameter and zeta potential, in both water and physiological salt solution (PSS). This was conducted using the Malvern ZetaSizer Nano ZS (Malvern, UK) which uses dynamic light scattering to analyse hydrodynamic diameter as well as being able to measure zeta potential.

10µL of the original nanoparticle solution is diluted into 1mL of distilled water and added into the relevant cuvettes to take the measurements. A standard Malvern cuvette is used to measure the size by dynamic light scattering, and a capillary cell, which has electrodes on either side, is used to measure the zeta potential of the sample.

2.7 Calculation of nanoparticle number and dosage

To determine concentration of stock nanoparticle solution, weight of a single nanoparticle was determined by rearranging the density equation:

$$(1)\ density\ of\ material = \frac{mass\ of\ one\ nanoparticle}{volume\ of\ one\ nanoparticle}$$

$$(2)\ mass\ of\ one\ nanoparticle = \ density\ \times volume\ of\ one\ nanoparticle$$

Where the volume of one nanoparticle is calculated using the equation for the volume of a sphere, under the assumption that the nanoparticle is perfectly spherical, and the density is the assumed density of the material used, so in this instance, silica or cerium oxide.

Once mass of one nanoparticle was calculated, 1mL of the stock solution of nanoparticles was dried and weighed. This mass was then divided by the mass of one nanoparticle calculated previously, and this determined how many particles per 1mL of stock solution there was.

2.8Results& Discussion

2.8.1 Silica nanoparticles

2.8.1.1 Size and morphology of dye-encapsulated silica nanoparticles using reverse microemulsion

With nanoparticles, the ideal characteristics include: spherical nature, monodispersed, with all the nanoparticles being of the same size, and no aggregation or clumps seen.

With the silica nanoparticles produced using the SilA and SilB method, the product proved undesirable as there was aggregation, as seen in Figure 4, when observed under electron microscopy and there was no clear distinction of individual nanoparticles. Because of this, another method was suggested as to produce a more desirable product that did not have aggregation and were more spherical in nature.Our aim is to produce nanoparticles that are able to be readily taken up by the vasculature with good physicochemical properties that allow for beneficial interaction with endothelial cells.

Characterisation of the silica nanoparticles was not conducted on samples produced using the reverse microemulsion method (SilA and SilB method) as the product was deemed unsuitable for this project and its use was discontinued.

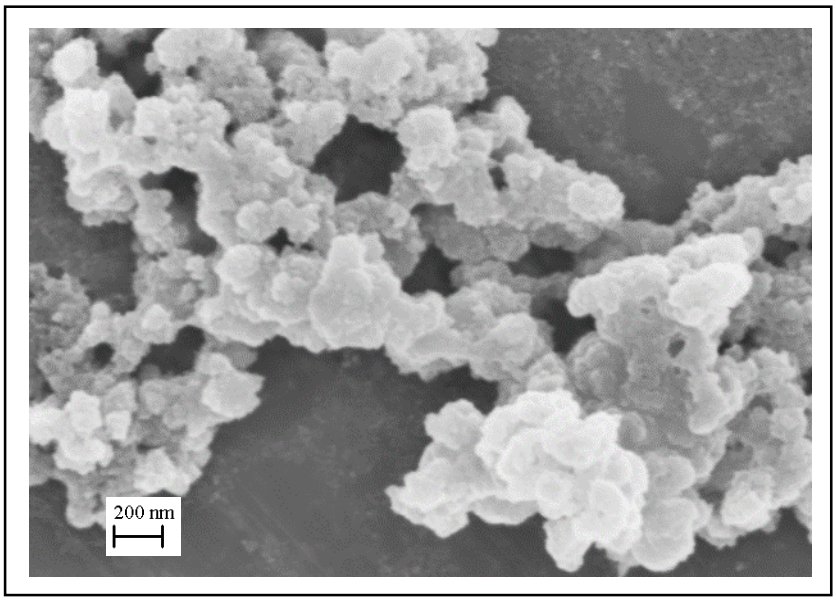

Figure 4SEM image of silica nanoparticles made using reverse microemulsion (SilA method)

2.8.1.2 Size and morphology of non-dye-encapsulated silica nanoparticles

Using a modified Stober method (SilC method), two batches of nanoparticles were produced following the same protocol, however, differences in size can be seen in Figure 5A and 5B (approximately 120 nm and 70nm in diameter, respectively). These differences highlight the sensitive nature of nanoparticle production, one of the key issues in comparing nanoparticle research.

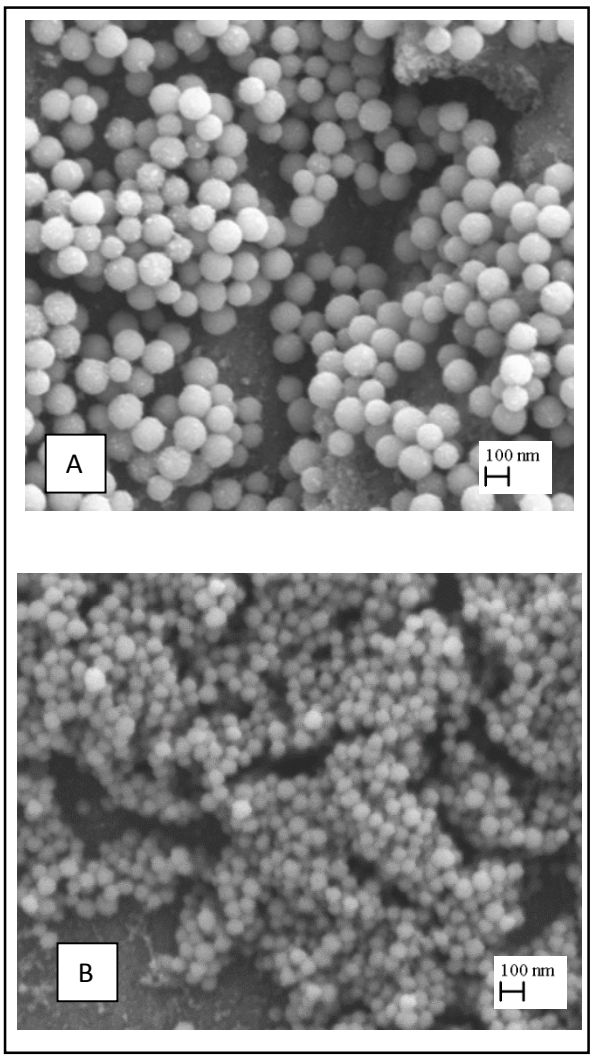

Figure 5SEM image of silica nanoparticles made using a modified Stober method (SilC method). A: SilC2; B: SilC3

2.8.1.3 Physicochemical characterisation of non- dye-encapsulated silica nanoparticles

Physicochemical characterisation was conducted and the techniques adopted include analysing hydrodynamic diameter and zeta potential, in both water and physiological salt solution (PSS). This was conducted using the Malvern ZetaSizer Nano ZS (Malvern, UK) which uses dynamic light scattering to analyse hydrodynamic diameter as well as being able to measure zeta potential. Size of the nanoparticles were also calculated using the SEM images (Figure 2), taking an average of 9 nanoparticle sizes. This sample size of 9 was chosen as it was the maximum amount of size measurements that can be taken electronically using the software provided. Manual measurements, although an option, would be less accurate.

The physicochemical characterisation for nanoparticles produced using the SilC method are listed in Table 2. Listed there is also the average size calculated from the SEM images, and a difference can be seen in the average size of the nanoparticles when comparing the two samples.

The hydrodynamic diameter does differ between suspension in water and suspension in PSS. This is because there are ions present in the PSS that interact with the surface charge of the nanoparticle and therefore alter its hydrodynamic diameter.The diameter in PSS is therefore expected to be larger than in water, contrary to our findings.

The zeta potential also changes when ions are present and this often leads to more unstable values being obtained for nanoparticles suspended in PSS. As mentioned previously, a zeta potential value of less than -25mV or greater than +25mV is considered stable(NanoComposix 2012). In Table 4, the values obtained from the nanoparticles suspended in water show high stability whereas the values obtained from the nanoparticles suspended in PSS show instability.

Table 4 Characterisation of silica nanoparticles produced by the modified Stober method (SilC method)

	Silica nanoparticles (SilC2)	Silica nanoparticles (SilC3)
Average SEM diameter (nm)	117.85	70.64
Hydrodynamic diameter in water (nm)	230.5	176.1
Hydrodynamic diameter in PSS (nm)	161.3	108.4
Zeta Potential in water (mV)	-104mV ± 17.4	-74.9mV ± 28.2
Zeta Potential in PSS (mV)	-22.6	-15.3

2.8.1.4 Size and morphology of dye-encapsulated silica nanoparticles

The silica nanoparticles, produced using the A3 methodology, are shown in Figure 6 and can be seen to be of a spherical nature with some variations in morphology seen. They were monodispersed and did not show aggregation.

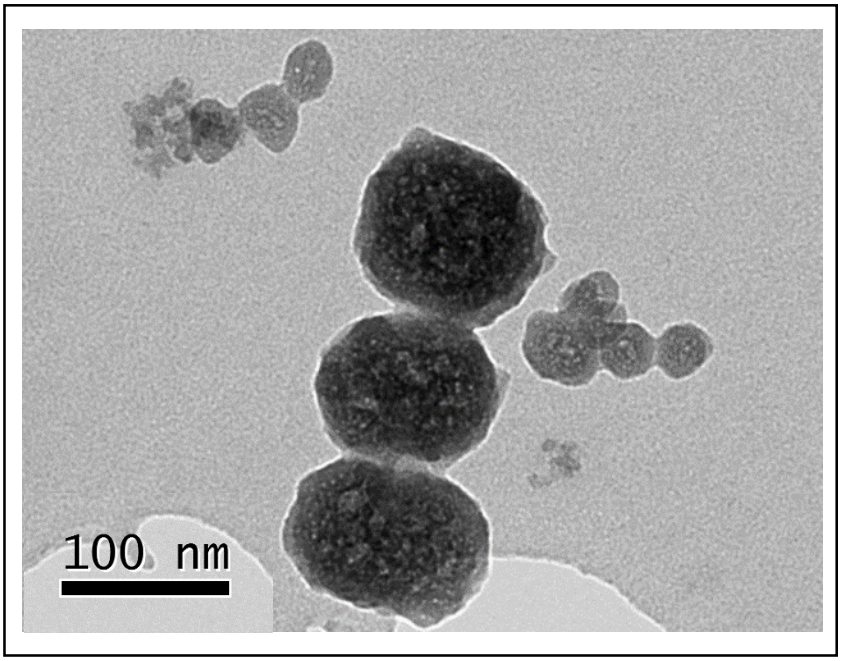

Figure 6 TEM image of silica nanoparticles produced using A3 method

The physicochemical characteristics for the silica nanoparticles (A3) are detailed in Table 5. Their hydrodynamic diameter seems to be smaller when suspended in PSS than in water. The zeta potential shows stability in water and instability in PSS as shown also in our synthesised silica nanoparticles. Sample A3 shows evidence of nucleation. This may be due to the length of time that the nanoparticles have been suspended in solution (approximately 1 year).

Table 5 Physicochemical characteristics of silica nanoparticles produced using the A3 method

	Silica nanoparticles (A3)
Average TEM size (nm)	98
Hydrodynamic diameter in water (nm)	141.83
Hydrodynamic diameter in PSS (nm)	124.1
Zeta Potential in water (mV)	-34.5
Zeta Potential in PSS (mV)	-12

2.8.2Ceria nanoparticles

2.8.2.1 Size and morphology of ceria nanoparticles

Previous studies suggest that ceria nanoparticles have a tendency to aggregate when synthesised(Rodea-Palomares, Boltes et al. 2011). This could possibly be due to the formation process of ceria nanoparticles where smaller nanoparticles cluster together to form aggregates, or it could be attributed to the physicochemical properties of the ceria nanoparticleswhich cause them to aggregate. In Figure 7, is the ceria nanoparticle sample made using the CeA method. This method produced ceria nanoparticles that contained aggregates over 200nm, and all varying in size and shape, although individual nanoparticles can also be visualised. Size and morphology was difficult to attain through the TEM images due to the individual nanoparticles being of such small size. Nanoparticles made using the CeA and CeB(seen in Figure 9A) method were deemed unsuitable, due to the high amount of aggregation.

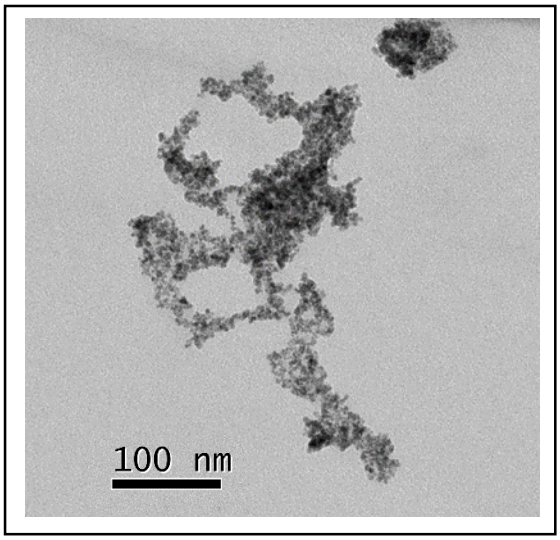

Figure 7TEM image of ceria nanoparticles produced using CeA Method

2.8.3 Post nanoparticle synthesis-steric stabilisation of ceria nanoparticles, using PVP, to look at effect of stabilisation on size, morphology and physicochemical characteristics

2.8.3.1 Size and morphology of Sigma ceria nanoparticles (steric and non-steric stabilised)

Steric stabilisation is a technique often used to help reduce aggregation by modifying or coating the surface of the nanoparticle. In doing so, it alters their physicochemical characteristics to allow fewer aggregates to form.

Polymer coating using Polyvinylpyrrolidone (PVP) was investigated using cerianano particles purchased from Sigma Aldrich as well as ceria nanoparticles produced from the CeB method. These were chosen as they were the most aggregated of the ceria samples produced and it was unclear if PVP coating could be done after the production of the ceria nanoparticles.

The ceria nanoparticles purchased from Sigma, although advertised as being less than 25nm, are shown to have particles around 50 and 100nm as well as those being under 25nm, as shown in Figure 8A. Along with the variation in size, there is also a variation in morphology, as some of the larger nanoparticles are of a square shape whereas the smaller nanoparticles are of a pentagonal or hexagonal shape. These nanoparticles were deemed unsuitable for use.

When coated with PVP, there is aggregation of the smaller particles, which can be seen in Figure 8B.

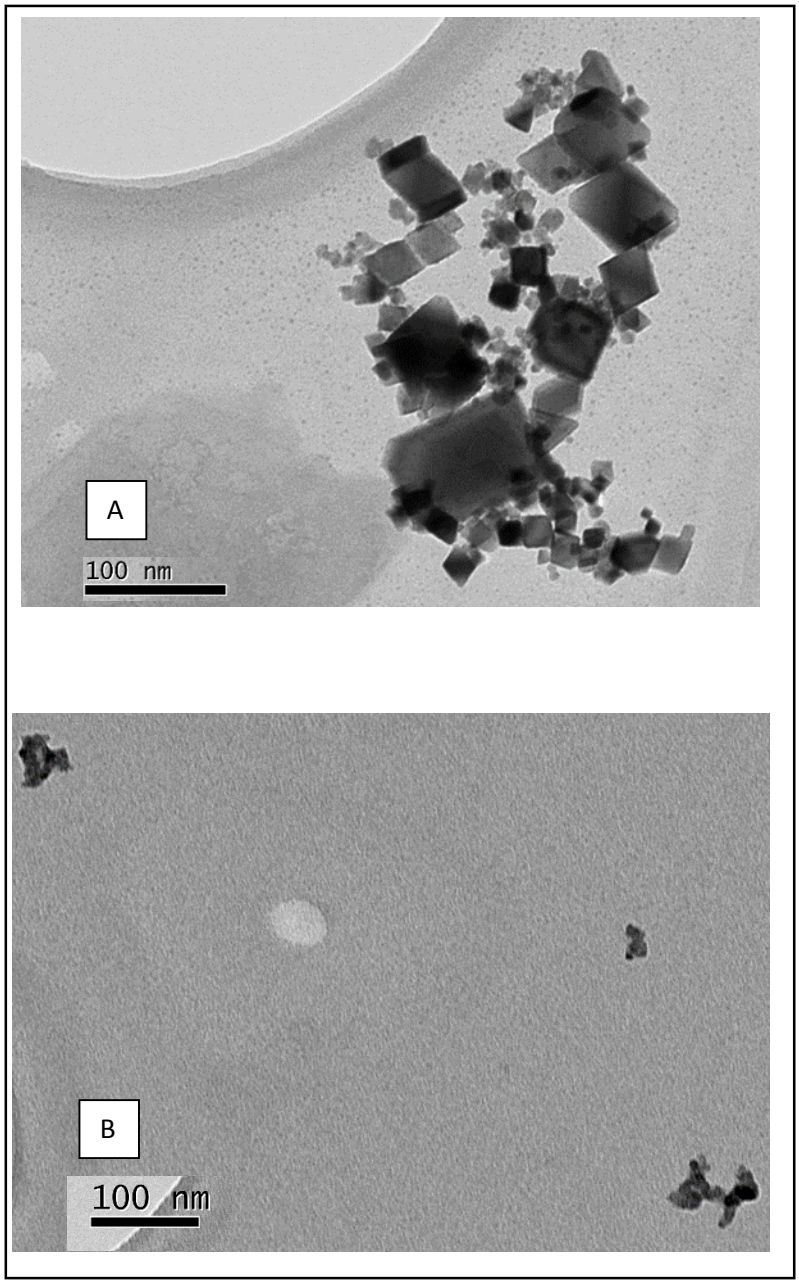

Figure 8 TEM image of ceria nanoparticles purchased from Sigma Aldrich depicted in (A) and same sample of nanoparticles after PVP coating (B)

2.8.3.2 Physicochemical characteristics of sigma ceria nanoparticles (steric and non-steric stabilised)

When looking at the physicochemical characerisation of the ceria nanoparticles purchased from Sigma, in Table 6, the hydrodynamic diameter increases dramatically when comparing the nanoparticles in water and in PSS. This is again understandable as the ions in PSS interact with the nanoparticles and contribute to the increase in hydrodynamic diameter. When PVP coating is added and the nanoparticles are suspended in water, there is an increase in hydrodynamic diameter. However, there seems to be an opposite effect when the nanoparticles are in PSS. The PVP coating reduces the hydrodyamic diameter of the nanoparticles when exposed to ions in the PSS. Looking at the zeta potential values, the PVP coating causes nanoparticle instability in both water and PSS. The reason for the lack of stabilisation in the Sigma ceria nanoparticles when coated with PVP remains unclear, but maybe related to insufficient coating of the NP surface.

Table 6 Physicochemical characterisation of Sigma ceria nanoparticles with and without addition of PVP coat

	Sigma ceria Nanoparticles (CeSig)	PVP coated Sigma ceria nanoparticles (CeSigPVP)
Hydrodynamic Diameter in water (nm)	235.8	623.2
Hydrodynamic diameter in PSS (nm)	$3.2x10^4$	2040
Zeta Potential in water (mV)	-25±4.2	-0.401
Zeta Potential in PSS (mV)	-12.6	-1.46

2.8.3.3 Size and morphology of ceria (CeB) nanoparticles (steric and non-steric stabilised)

The ceria nanoparticles produced using the CeB method, as previously mentioned, had high levels of aggregation, as seen in Figure 9A, and varied in size and morphology. Figure 9B shows the same CeB nanoparticle sample after coating with PVP. Smaller clusters of nanoparticles can be seen, of much smaller size than the aggregates seen in Figure 9A, that did not have the PVP coating.

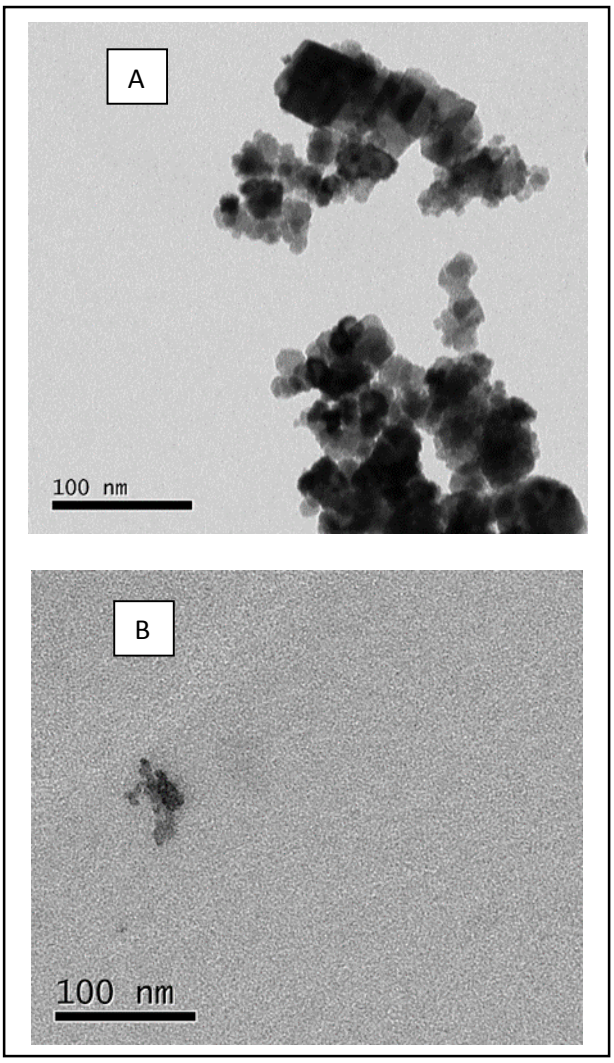

Figure 9 TEM image of ceria nanoparticles produced using CeB method depicted in (A) and the same sample of nanoparticles after PVP coating (B)

2.8.3.4 Physicochemical characteristics of ceria (CeB) nanoparticles (steric and non-steric stabilised nanoparticles)

When looking at the physicochemical characterisation of these ceria nanoparticles (seen in Table 7), with and without the PVP coating, the PVP coating aids in reducing the hydrodynamic diameter both when the nanoparticles are suspended in water and PSS, as well as producing a more stable zeta potential.

Table 7 Physicochemical characterisation of ceria nanoparticles produced using CeB method, with and without PVP coating

	Ceria nanoparticles (CeB2)	PVP coated ceria nanoparticles (CeB2PVP)
Hydrodynamic diameter in water (nm)	1750	503.3
Hydrodynamic diameter in PSS (nm)	2410	742
Zeta Potential in water (mV)	-0.242	-4.5
Zeta Potential in PSS (mV)	-1.56	-12.1

2.8.4 Steric stabilisation amid ceria nanoparticle synthesis using PVP

As well as applying a PVP coat to ceria nanoparticles, two methods were used that incorporated the PVP along with the starting materials for ceria nanoparticle production. This was due to the fact that, although PVP coating was able to bring about a slightly more stable suspension of nanoparticles, the nanoparticles were still highly aggregated. By introducing the PVP along with the starting materials, there is a high probability of coating individual nanoparticles as they are formed and before they adhere to one another.

2.8.4.1 Size and morphology of steric stabilised ceria (CeE) nanoparticles

PVP coated ceria nanoparticles produced using the CeE method, show individual nanoparticles with pentagonal and hexagonal morphology, as seen in Figure10. Although there is agregation seen and the ceria nanoparticles retain their tendency to adhere to one another, the PVP coat has enabled the formation of individual nanoparticles.

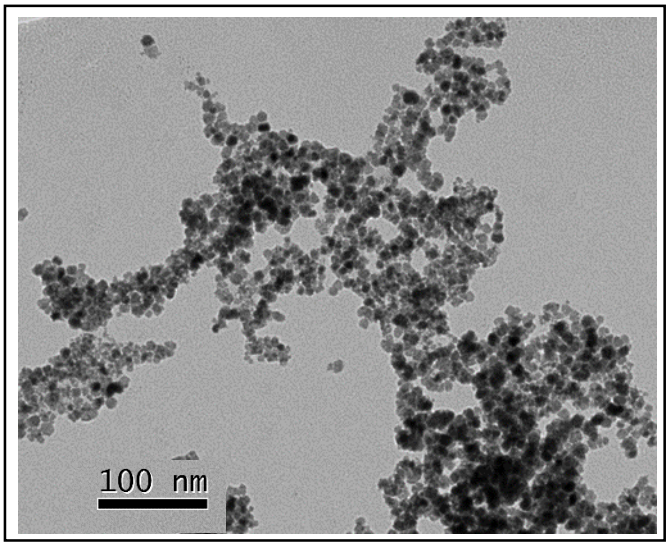

Figure 10 TEM image of PVP coated ceria nanoparticles produced using the CeE method

2.8.4.2 Physicochemical characteristics of steric stabilised ceria (CeE) nanoparticles

When looking at the physicochemical characterisation of these nanoparticles, in Table 8, the hydrodynamic diameter values calculated show high levels of aggregation in both water and PSS. Despite the PVP coating allowing for individual nanoparticle formation, it did not contribute to reducing aggregation. The zeta potential values obtained for the nanoparticles suspended in water and PSS, indicate high instability and therefore would not be a desirable product to be used in this project.

Table 8 Physicochemical characterisation of PVP coated ceria nanoparticles produced using CeE method

	PVP-coated ceria nanoparticles (CeE1)
Hydrodynamic diameter in water (nm)	2908
Hydrodynamic diameter in PSS (nm)	1172
Zeta Potential in water (mV)	-2.3
Zeta Potential in PSS (mV)	-1.78

2.8.4.3 Size and morphology of steric stabilised ceria (CeF) nanoparticles

The CeF method was also used, which incorporated PVP into the starting materials. The difference with this method is that it did not have water as the solvent, instead it used ethylene glycol. This aids in producing individual nanoparticles of a more spherical nature, as demonstrated by Figure 11. Although variation in size is still seen (ranging from approximately 20nm to 50nm), the nanoparticles are much more defined in their shape.

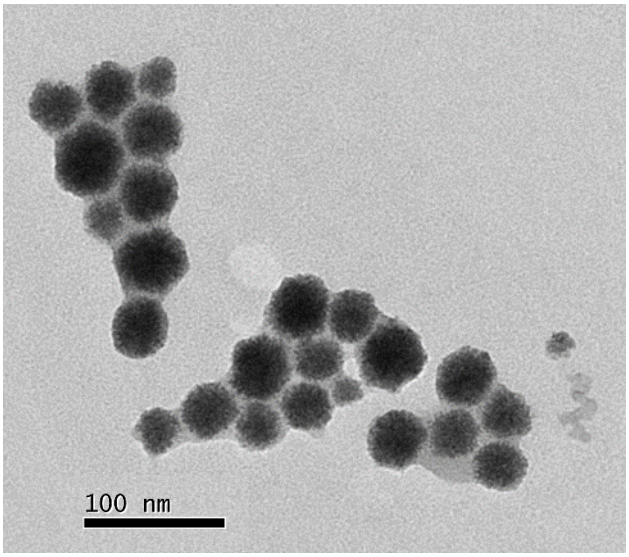

Figure 11 TEM image showing ceria nanoparticles coated with PVP using CeF method

2.8.4.4 Physicochemical characteristics of steric stabilised (CeF) nanoparticles

The physicochemical characterisation for the ceria nanoparticles made using the CeF method, are listed in Table 9. The hydrodynamic diameter shows high levels of aggregation when nanoparticles are suspended in PSS. The zeta potential for nanoparticles suspended in water and in PSS show instability, however, this may be due to a minute amount of ethylene glycol still present in the sample.

Table 9Physicochemical characterisation of ceria nanoparticles produced using the CeF method

	Ceria nanoparticles (CeF1)
Hydrodynamic diameter in water (nm)	245.8
Hydrodynamic diameter in PSS (nm)	569.3
Zeta potential in water (mV)	-15±5.82
Zeta potential in PSS (mV)	-5.32

2.8.5 Steric stabilisation amid ceria nanoparticle synthesis using dextran

Dextran, a polymer made up of glucose molecules, has been used to coat nanoparticles and have been shown previously to be able to coat ceria nanoparticles without interfering with the antioxidant properties as well as enhanced uptake into endothelial cells(Perez, Asati et al. 2008).

2.8.5.1 Size and morphology of steric stabilised ceria (CeG) nanoparticles

Dextran coated ceria nanoparticles were made using the CeG method. In this method, the dextran is incorporated along with the starting materials. In Figure 12, the dextran coated ceria nanoparticles are seen to be very small and clumped together. It is evident that the nanoparticles are too small to be analysed properly, therefore size and morphology could not be conducted on this sample.

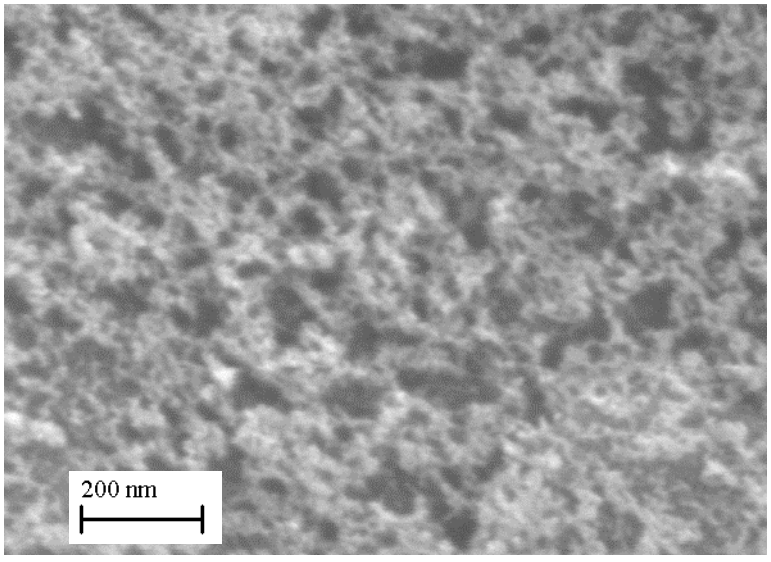

Figure 12SEM image of ceria nanoparticles coated with dextran using the CeG method

2.8.5.2 Physicochemical characteristics of steric stabilised ceria (CeG) nanoparticles

The physicochemical characterisation for the dextran coated ceria nanoparticles are listed in Table 10. The hydrodynamic diameters collected show that aggregation is present and the zeta potential values do show slight instability in both water and in PSS.

Table 10 showing the characterisation for the dextran coated nanoparticle sample (CeG1)

	Ceria nanoparticles (CeG1)
Hydrodynamic diameter in water (nm)	1032
Hydrodynamic diameter in PSS (nm)	284.3
Zeta Potential in water (mV)	-18.6
Zeta Potential in PSS (mV)	-16.1

2.8.6 Ceria-coated silica nanoparticles

2.8.6.1 Size and morphology of ceria-coated silica nanoparticles

These nanoparticles were produced using the ceria precursor produced from the CeA method and the silica nanoparticles produced from the SilC method, following the method outlined in (Oh, Lee et al. 2010). In Figure 13, it can be seen that the ceria nanoparticles are coated onto the silica nanoparticle surface.

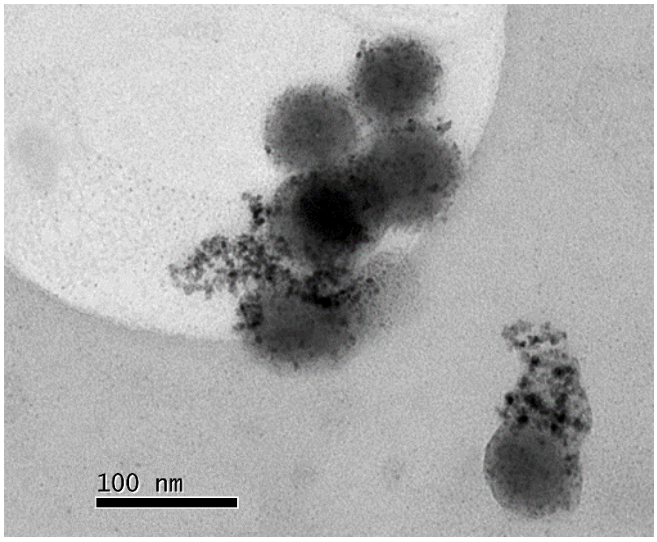

Figure 13 shows the TEM image for the ceria coated silica nanoparticles

2.8.6.2 Physicochemical characteristics of ceria-coated silica nanoparticles

The physicochemical characterisation of the ceria coated silica nanoparticles are listed in Table 11. The hydrodynamic diameter, both when the nanoparticles are suspended in water and in PSS, show aggregation, although this may be due to the presence of ceria on the silica nanoparticles' surface. The zeta potential values, in both water and PSS, show instability.

Table 11 shows the characterisation for the ceria coated silica nanoparticle (SilC3Ce1)

	Ceria coated silica nanoparticles (SilC3Ce1)
Hydrodynamic diameter in water (nm)	8042
Hydrodynamic diameter in PSS (nm)	367.5
Zeta Potential in water (mV)	-14.1
Zeta Potential in PSS (mV)	-5.45

3. Objective 2: Vascular Functional Studies

3.1 Methodology

3.1.1. Organ bath studies

C57/BLACK 6 mice were used for this project, of two age groups:7 young mice aged between 10-19 weeks, and7 aged mice aged between 74-106 weeks. Not all data is included for all of these animals as some were used to optimise the equipment used.Animals were sacrificed by cervical dislocation of the neck, in accordance with institutional guidelines and the Scientific procedures act, 1986 (Schedule 1) and ethics approval. The heart and lungs, along with the connecting vessels were removed enblock and the aorta was then dissected away and any fat removed. Aortas were cut into aortic rings of 3mm in length. These aortic rings were then mounted onto a calibrated organ bath system, as shown in Figure 14. Physiological conditions were set, by immersing in oxygenated (95% oxygen; 5% CO2) physiological salt solution [PSS], of the following composition: 119 NaCl, 4.7 KCl, 1.2 $MgSO_4 \cdot 7H2O$, 25 $NaHCO_3$, 1.17 $KHPO_4$, 0.03 K_2EDTA, 5.5 glucose, and 1.6 $CaCl_2 \cdot 2H2O$; pH

7.4.Solutions were maintained at 35˚C.

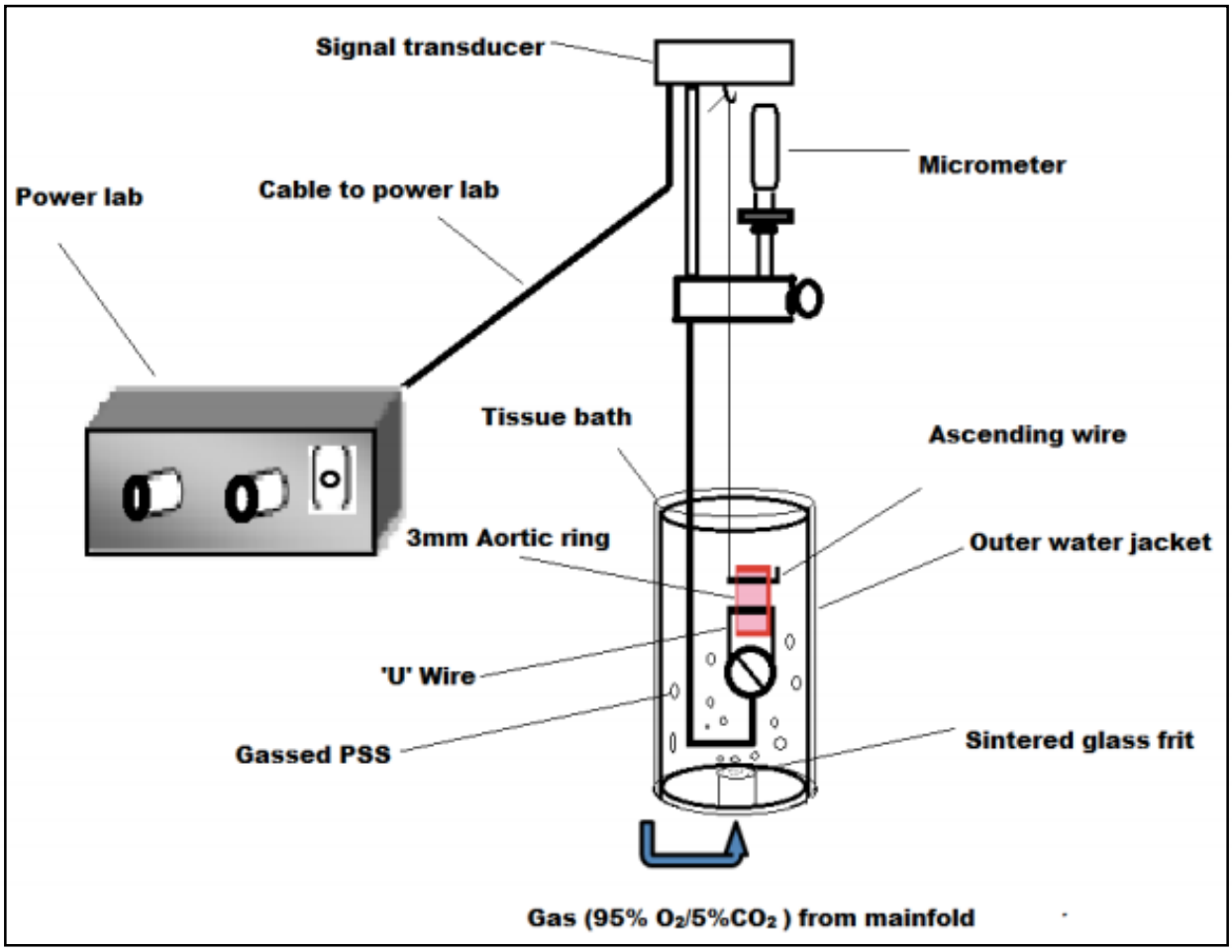

Figure 14Schematic showing the organ bath system(taken from Akbar, et al. 2011)

The organ bath system was initially calibrated as detailed in the appendix. Once mounted into the organ bath system, aortic rings from both young and aged groups underwent the same protocol, which is outlined in Figure 15.Constrictor responses were examined using high potassium PSS (KPSS) solution and Phenylephrine (Phe). Acetylcholine was used to assess endothelial-dependent dilation, whilst sodium nitroprusside was used to assess endothelial-independent dilation.

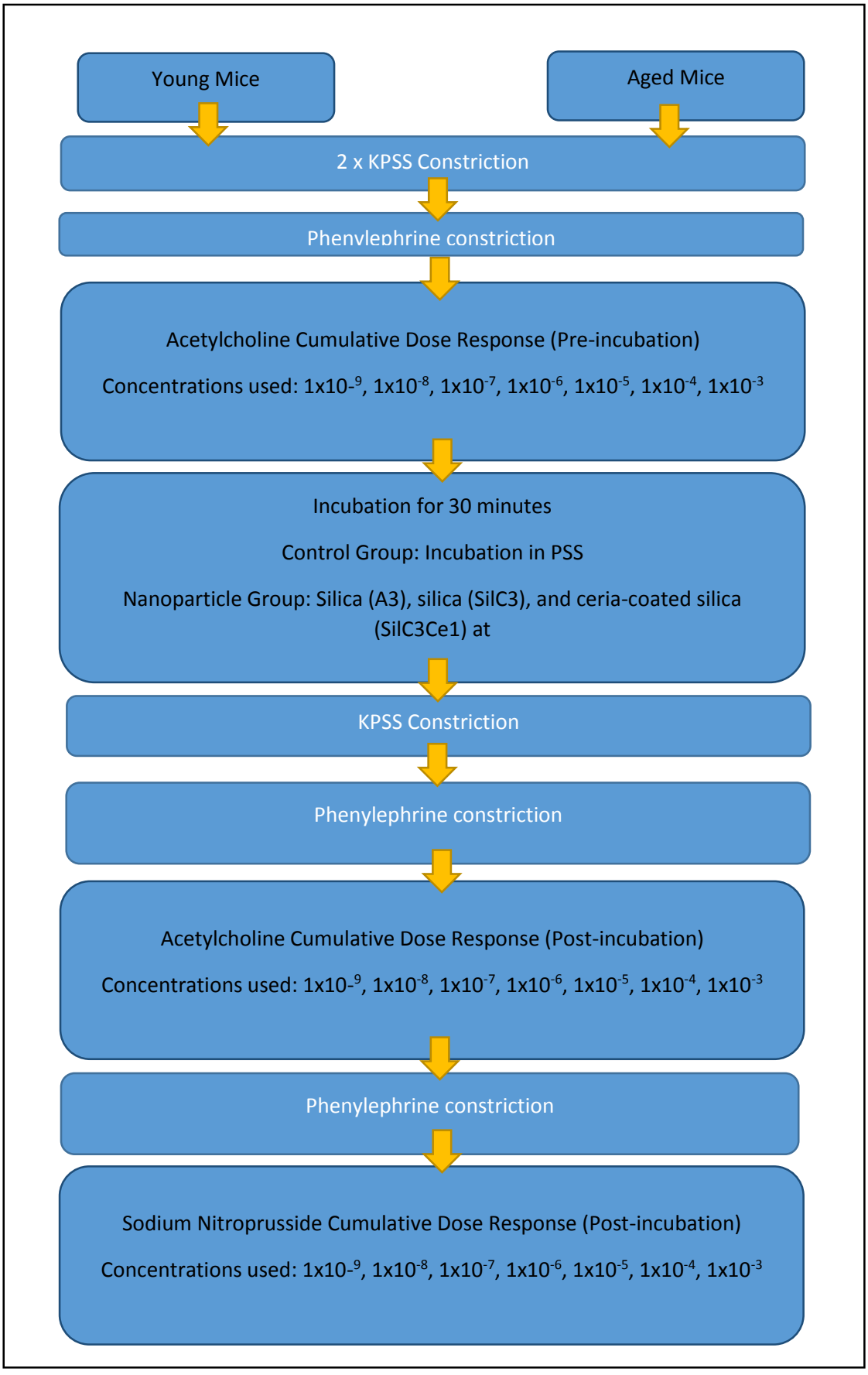

Figure 15 Schematic showing the protocol for the organ bath experiments

For the control group, vessels were incubated in PSS over 30 minutes and reconstricted. The Ach and SNP cumulative dose responses were repeated. The vessel again constricted and an SNP cumulative dose response carried out. At the end of the experiment, the vessel was washed in PSS.

To assess the influence of nanoparticles on constrictor and dilator responses, vessels were incubated in any one of the following nanoparticles for 30 minutes, washed, then reassessed using cumulative doses of Ach, and SNP:

For all the nanoparticles above vessel incubation was made to a final dosage of 1.31 x 10^{11} NP/ml in a 15mL organ bath. The amount added was calculated using the C1V1=C2V2 equation, as the concentration of the stock solution of nanoparticles was already calculated, as previously mentioned.

3.1.2 Interpreting raw data from organ bath studies

The raw data, known as traces, consist of tension values obtained through contraction and dilation of the aortic ring. From these tension values, the percentage dilation from each cumulative dose response was calculated and a response curve was generated. Percentage dilation was calculated using the following formula:

$$Percentage\ dilation = \frac{change\ in\ tension\ during\ dilation}{starting\ tension} \times 100\%$$

Two chemicals were used to induce endothelial dilation in the aortic rings. Acetylcholine (Ach)was used to induce endothelial-dependent dilation, and sodium nitroprusside (SNP)was used to induce endothelial-independent dilation.

3.1.3 Tissue fixation and TEM

At the end of an experiment, some vessels were immediately fixed in 2.5% glutaraldehyde in 0.1Msodium cacodylate buffer, pH 7.3 over 2 H at 22◦C, then kept in cacodylate buffer until processed for transmission electron microscopy (TEM) at the university of manchester (UoM). Ultrathin 70 nm sections were cut with Leica “Ultracut S” ultramicrotome and placed on copper grids by the technical staff. The grids were observed (using the Tecnai 12 Biotwin TEM at 80 kV) at UoM.

3.1.4 Statistical analysis for organ bath data

Data are given as mean ± standard error of mean with *n* representing
the number of rats/vessels. Dilator responses are expressed
as percent relaxation.

For analysing the repeatability of the vasodilator responses, a paired t-test was conducted, as it was an analysis before and after an incubation, using the same vessel. This statistical analysis was conducted using IBM SPSS software.

For analysing the nanoparticle influence on vasodilator responses, a one-way ANOVA was conducted with Bonferroni and Tukey post-hoc tests. This was chosen as it was a comparison of more than two experimental conditions and was not conducted on the same vessel.

3.2 Results& Discussion

3.2.1. Constrictor responses in young mice

Preliminary results were conducted to establish the resting tension necessary to achieve the highest constrictor response, using Phe. Tensions of 0.1; 0.2; 0.3; 0.4; and 0.5 g tensions were tested, the data for which, can be found in the appendix. Vessels set up at 0.4g tension achieved the highest Phe constrictor response. Therefore, vessels were set up at 0.4g tension, as the resting tension of the vessel.

During the experiment protocol, vessels were initially induced to contract using 15mL ofKPSS. This established the viability of the vessels. This step was repeated 2 times. Vessels reaching less than 0.16 g tension were discarded. Vessels were subsequently constricted using Phe at a final bath concentration of 1mM before the cumulative dose response for Ach is conducted. The average tension values for responses to KPSS and Phe are given in Table 12 below.

Table 12 Average tension achieved using high potassium PSS and phenylephrine in young mice

	Average tension achieved (g)± SD
High potassium PSS	0.33 ± 0.10
Phenylephrine	0.25 ± 0.14

3.2.2 Constrictor responses in aged mice

Vessels from the aged mice were also induced to contract using a high potassium PSS, and a $1x10^{-3}$dose of phenylephrine. The average tension achieved in the initial contraction,before the acetylcholine dose response (pre incubation), can be seen in Table 13.

Table 13 Average tension achieved using high potassium PSS and phenylephrine in aged mice

	Average tension achieved (g) ± SD
High potassium PSS	0.58 ± 0.38
Phenylephrine	0.48 ± 0.18

3.2.3 Repeatability of acetylcholine dilator responses in young mice

All vessels dilate when acetylcholine is present, and it dilates in a dose-dependent manner. It is this dose response that is used in the comparisons. Assessing the repeatability of the acetylcholine dilator response before and after a PSS incubation enables us to investigate if the responses can be directly compared. In Figure 16, it can be seen that the acetylcholine response post incubation is significantly lower than the response achieved pre incubation ($p<0.01$, at 0.1µM to 1mM). Due to this, only post-incubation responses were compared when analysing nanoparticle influence on vasodilator responses.

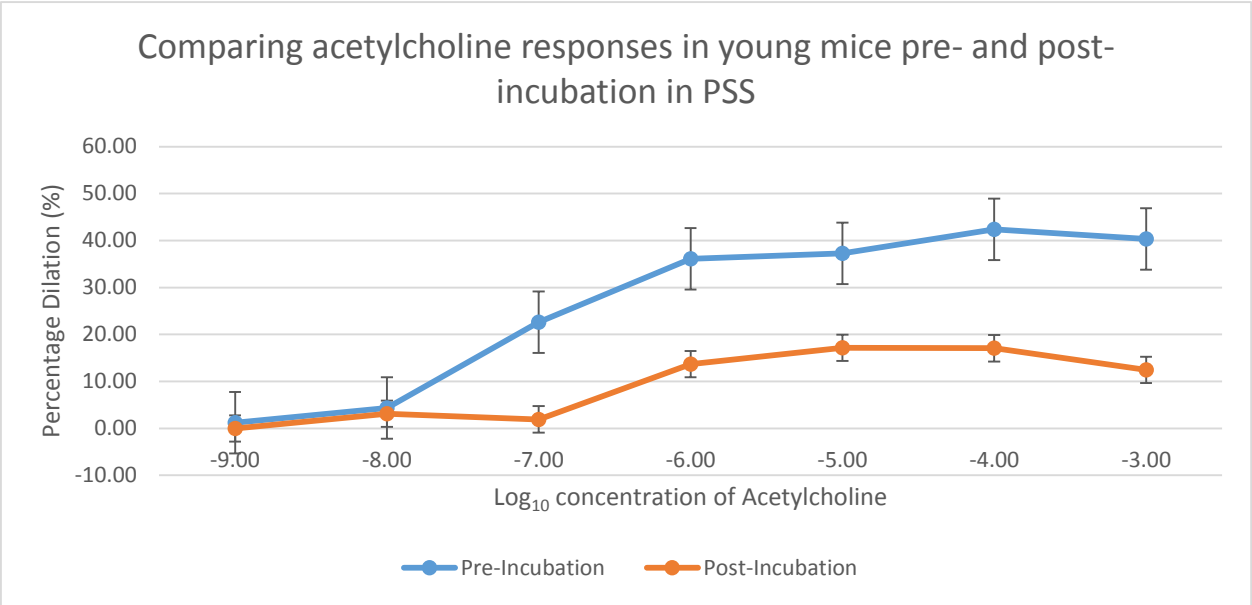

*Figure 16 Percentage dilation during an acetylcholine dose response before (n=10) and after (n=4) incubation in PSS. *p<0.05; **p<0.01.*

3.2.4The influence of age on acetylcholine dilator function

When looking at the acetylcholine dose response achieved from the young mice, in Figure 17, there can be seen that, with each increasing dose there is an increase in the dilation of the aortic ring. This dilation peaks at 45%, when the concentration of the acetylcholine reaches $1x10^{-4}$M and begins to have a slight contractile effect at concentration $1x10^{-3}$M. The acetylcholine dose response achieved in aged mice, also seen in Figure 14, also show an increase in dilation of the aortic ring with each increasing dose. The dilation peaks at almost 50% when the concentration reaches $1x10^{-6}$M, and remains relatively steady for subsequent concentrations.

When comparing the responses between the young and the aged, using statistical analysis, there was found to be no significant difference.

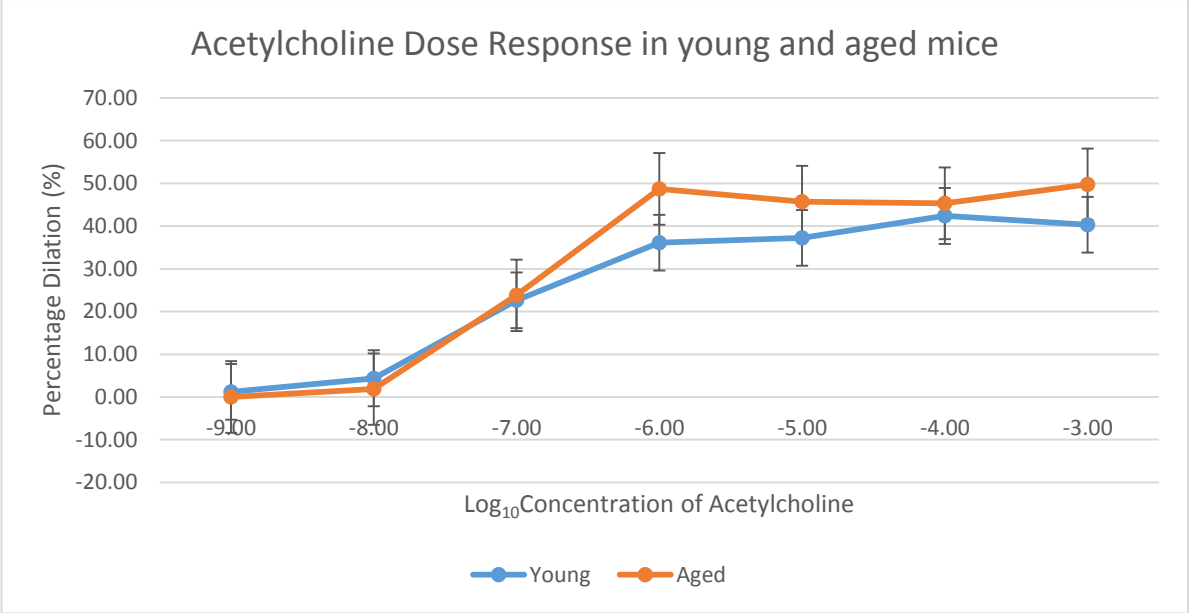

Figure 17 Comparison of the percentage dilation during an acetylcholine dose response in young(n=4) and in aged (n=3)

3.2.5The influence of nanoparticle incubation on acetylcholine dilator response in young mice

After incubation in nanoparticles, the aortic rings from young mice underwent another acetylcholine dose response, seen in Figure 18. Although the acetylcholine response shows a similar trend after each of the nanoparticle incubations, the ceria-coated silica nanoparticle incubation caused an increased dilator response than that seen after the silica nanoparticle incubation or the PSS incubation. Statistical analysis shows that the ceria-coated silica nanoparticle incubation caused a significant increase in dilator response at the concentration $1x10^{-7}$M when compared to the acetylcholine response after both the silica nanoparticle and PSS incubation($p< 0.05$). There was also no statistical difference seen when comparing the acetylcholine dilator response after silica nanoparticle incubation and PSS incubation.

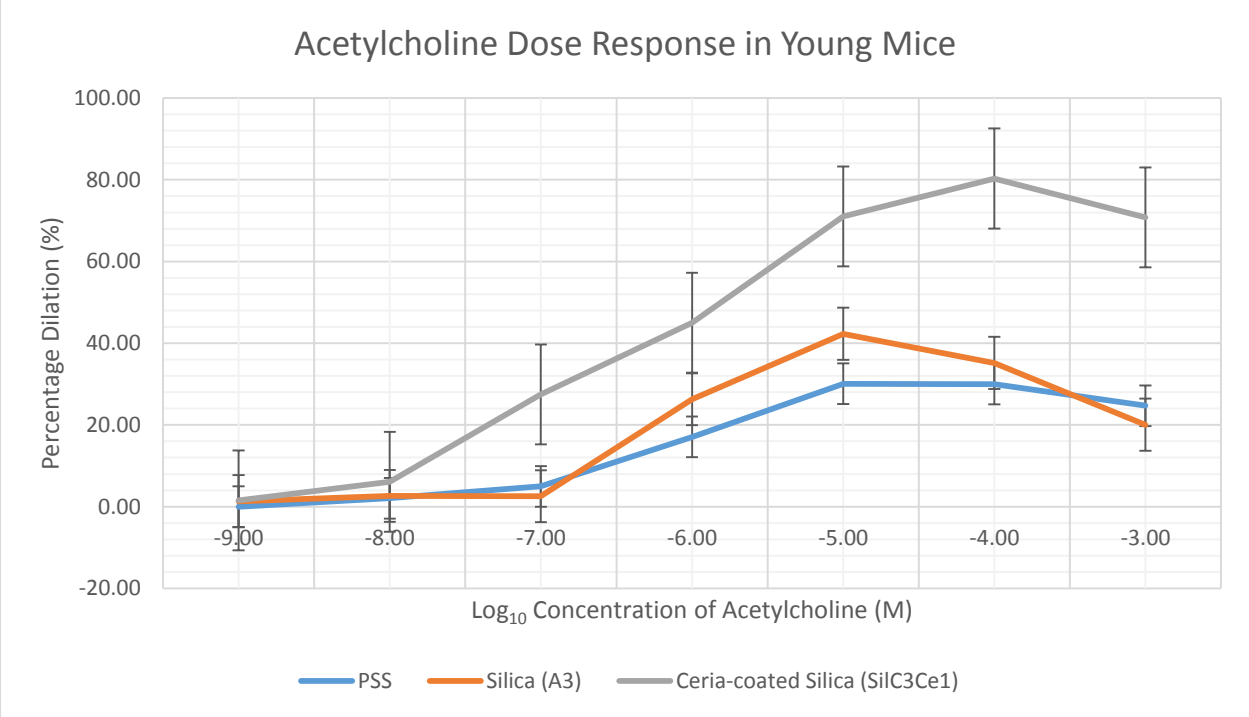

Figure 18 Percentage dilation during an acetylcholine dose response after incubation with either PSS (n=6), silica nanoparticles (A3) (n=4) or ceria-coated silica (n=3)

3.2.6 The influence of nanoparticle incubation on sodium nitroprusside dilator response in young mice

In Figure 19, it can be seen that the sodium nitroprusside response causes an increase in dilation percentage at each concentration, regardless of whether the aortic ring was incubated in silica or ceria-coated silica nanoparticles, or in PSS. The sodium nitroprusside responses after incubation with nanoparticles, both silica and ceria-coated silica, showed no statistically significant difference to the controls.

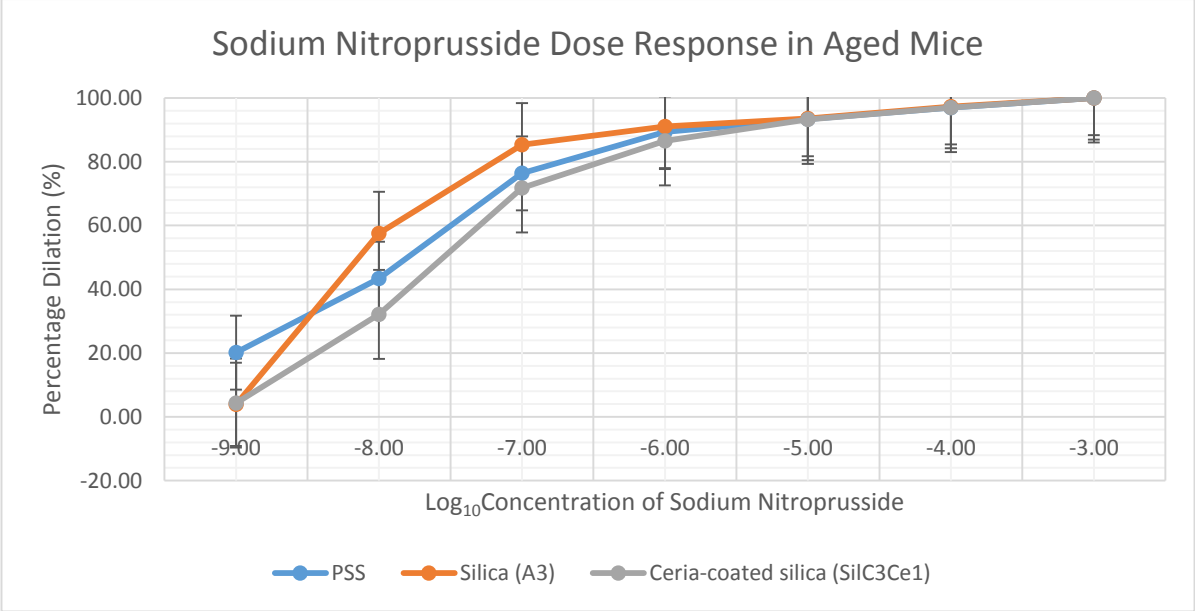

Figure 19 Percentage dilation during a sodium nitroprusside dose response after incubation with either PSS (n=6), silica nanoparticles (A3) (n=4) or ceria-coated silica (n=3)

3.2.7 The influence of nanoparticle incubation on acetylcholine dilator response in old mice

After incubation in nanoparticles, another acetylcholine dose response was conducted, seen in Figure 20. The acetylcholine dose response after incubation in silica (SilC3) and ceria-coated silica, show no difference when compared to the response after incubation in PSS. However, there is a detrimental effect to the acetylcholine dose response after incubation in silica (A3) nanoparticles when compared to the acetylcholine dose response after incubation with PSS. This was, however, also not found to be statistically significant.

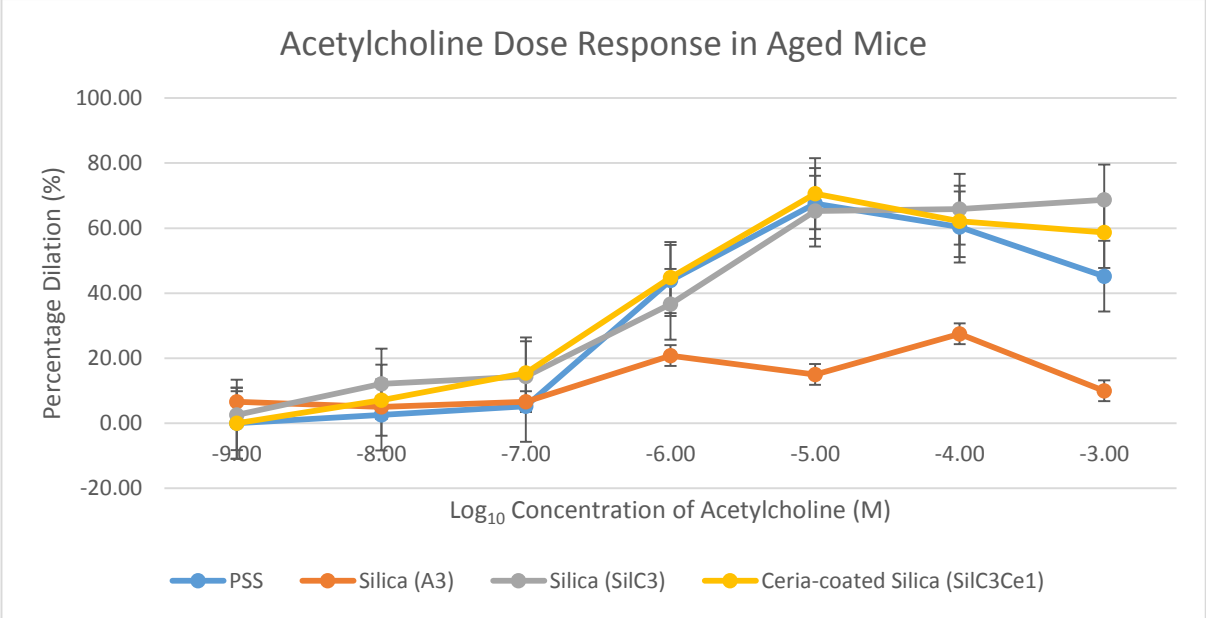

Figure 20 Percentage dilation during an acetylcholine dose response, in aged mice, post-incubation in either PSS (n=4), silica nanoparticles (Ali's A3) (n=2), silica nanoparticles (SilC3) (n=3), or ceria coated silica nanoparticles (n=3)

3.2.8 The influence of nanoparticle incubation on sodium nitroprusside dilator response in old mice

In Figure 21, it can be seen that the sodium nitroprusside response causes an increase in dilation percentage at each concentration, regardless of incubation. The sodium nitroprusside responses after incubation with nanoparticles, silica and ceria-coated silica, show no statistically significant difference to the controls.

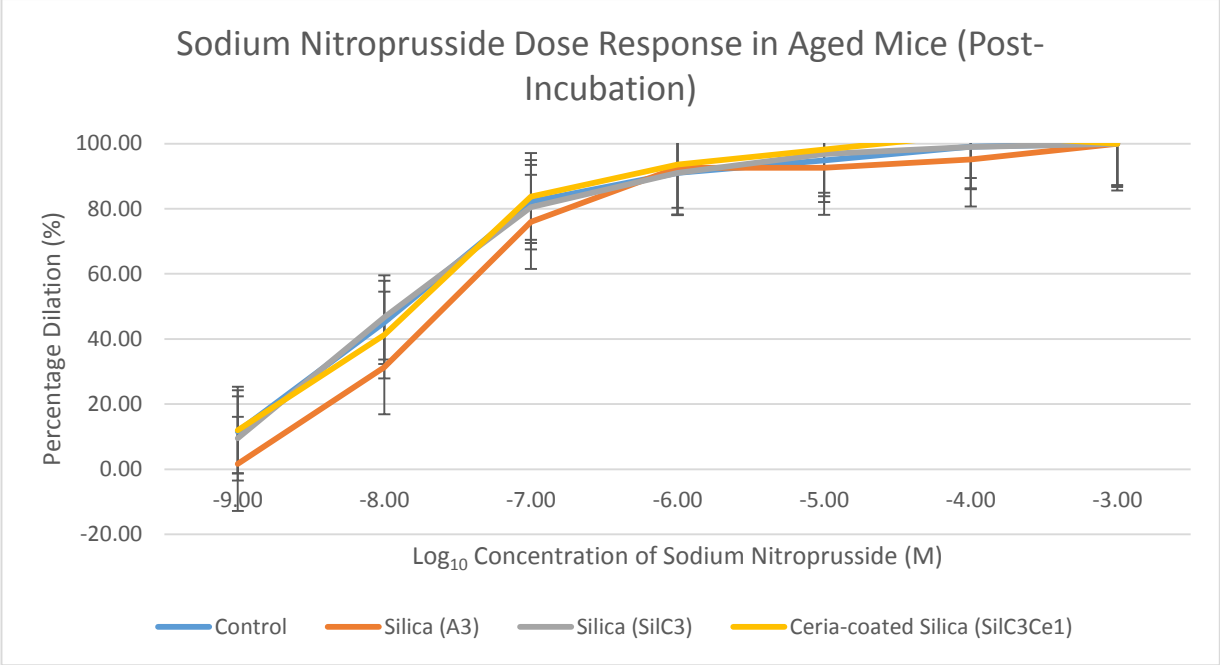

Figure 21 Percentage dilation during a sodium nitroprusside dose response post-incubation in either PSS (n=4), silica nanoparticles (Ali's A3) (n=2), silica nanoparticles (SilC3) (n=3), or ceria-coated silica nanoparticles (n=3)

3.2.9 Evaluation of uptake of nanoparticles using TEM

After fixation and processing, vessel tissue was cross sectioned and viewed using TEM. Difficulty in obtaining an intact endothelium meant analysis of uptake was unsuccessful, however some images of nanoparticles within the processed tissue can be seen in Figure 22.

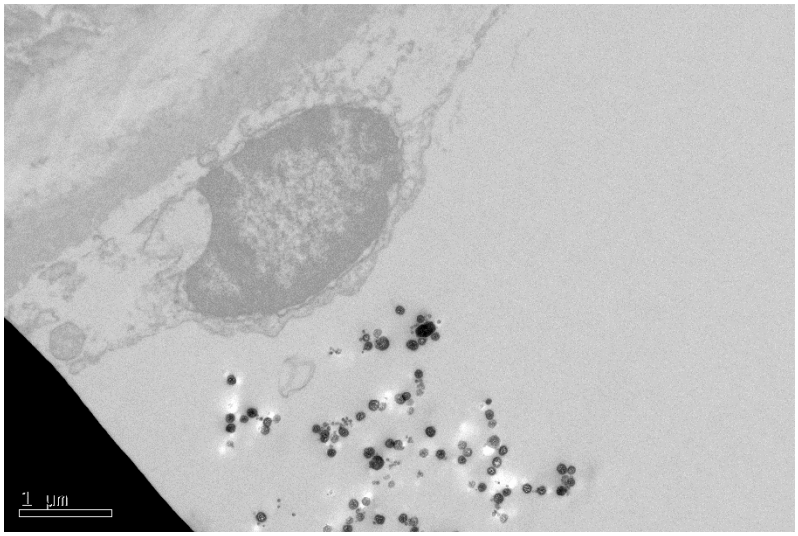

Figure 22 TEM image of silica (A3) nanoparticles surrounding an endothelial cell

4. General Discussion and Conclusion

4.1 Nanoparticle synthesis and characterisation

A number of methodologies were examined in the present study to synthesise monodispersed and spherical nanoparticles, of 2 different material compositions: Silica (3 methods) and Ceria (6 methods). These were compared to other nanoparticles, either already available in our lab (A3 Silica nanoparticles), or commercially available (Ceria nanoparticles from Sigma). Additionally, some of the silica nanoparticles were also coated in ceria, to produce 'ceria-coated silica nanoparticles'.

The nanoparticles synthesised showed a variation in physicochemical properties and therefore, those selected for the present study had to be comparable to one another, which is why the ceria-coated silica and silica (SilC3) nanoparticles were used for further vessel physiology testing. Comparisons were made to silica nanoparticles made previously in our lab (A3).

The present study demonstrates the successful synthesis of ceria nanoparticles of 20-50 nm in size (CeF1), by incorporation of PVP polymer into the starting material and using ethylene glycol instead of water as the solvent material. This overcame the high level of aggregation seen when using other methods of synthesis. However, use of PVP can prevent nanoparticle uptake into endothelial cells and tissues, as it has previously been used to enhance the circulation time of nanoparticles in blood(Duan and Li 2013). Although dextran (used to enhance nanoparticle uptake) was used as an alternative coating method to improve steric stability of the ceria nanoparticles, aggregation remained a problem. This may be due to the very small size of the ceria nanoparticles ….

Ceria coating of silica nanoparticles was achieved in the present study using the method previously described by Farooq, et al. 2014, who also looked at the restoration of dilator responses using ceria. Coating was confirmed by TEM analysis . Although most of the surface was covered, isolated aggregates of ceria nanoparticles alone was also seen. This may have contributed to the increased values of hydrodynamic diameter.

4.2 Do aged mice show compromised dilator responses to acetylcholine?

Aortic vessels from young and aged mice were isolated and maintained under conditions that mimic the physiological state. All vessels constricted to high potassium solution, demonstrating their viability. The results in the present study have found that there is no compromised endothelial dependent (Ach) dilator responses seen in aged mice when compared to young mice. The acetylcholine dose response achieved in young and aged mice, show no statistically significant difference. This was unexpected, since reduced dilator responses in aged vessels has previously been documented, due to reduced availability of nitric oxide(Yang, Huang et al. 2009). However, the present results are supported by the finding in our lab, that femoral arteries from the same aged mice, also showed similar dilator responses to those from young mice (Diaz et al, in preparation). The reason for this may be due to the possibility, that reduced nitric oxide levels may be compensated by other vasodilators such as EDHFs.

4.3 Do silica nanoparticles compromise dilator responses in young or aged mice?

Incubation of vessels in silica and ceria-coated silica nanoparticles had no overall effect on constrictor responses [Phe]. All vessels, from young and aged mice, demonstrated a dose dependent increase in endothelial independent dilator responses [SNP], after nanoparticle incubation, demonstrating that smooth muscle cell sensitivity was unaffected by the nanoparticles. However, changes were observed in endothelial dependent (Ach) dilation, after nanoparticle incubation, as follows: In young mice, the silica nanoparticles (A3) caused no overall change in dilator responses compared to the controls (figure 15) whereas in the aged mice, the same A3 silica nanoparticles caused a reduction in dilator responses (figure 17). Another type of silica nanoparticle (C3), however, showed no reduction in dilator responses in aged mice, indicating that the physicochemical characteristics can impact the biocompatibility. The reason why the A3 silica nanoparticles had a reduced effect on dilator capacity of old but not aged vessels, may relate also to the fact that the types of mediators released in aged vessels may be different from young vessels. A3 silica nanoparticles were dye encapsulated and we have demonstrated evidence in our lab that this can generate reactive oxygen species, thus interfering with nitric oxide release and leading to reduced dilation (Farooq et al, 2013). This is supported by the fact that in the present study, C3 silica nanoparticles (which do not contain the dye) did not reduce the dilator component in the aged vessels.

4.4 Can adding a ceria coat, improve dilator responses?

In young mice, there is an improvement in dilator responses seen after incubation with ceria-coated silica nanoparticles, however, no improvement is seen in the aged mice. This result is promising, but further studies are required in order to compare the ceria-coated silica nanoparticles with the bare silica nanoparticles without the ceria coat (C3). The present study confirms previous findings by Farooq et al (2014). They used aortic vessels from young male Wistar rats and demonstrated that incubation of vessels in silica nanoparticles alone caused a significant reduction in endothelial dependent dilation (Ach). Incubation in ceria coated silica nanoparticles, led to a significant improvement in dilation (Farooq et al, 2014). The authors suggest that as ceria is available in 2 oxidation states, it can behave as a reactive oxygen species scavenger, scavenging any ROS generated by the surface of the silica nanoparticles, which may have led to the original reduction in dilation (Farooq et al, 2014).

The additional finding, in the present study, is that ceria coating of silica nanoparticles does not improve dilation in the aortic vessels from aged mice. This is expected, since the uncoated silica nanoparticles (C3) had no detrimental effect on endothelial dependent dilator responses and the dilator component in aged vessels is uncompromised, compared to that in young vessels.

4.5.Future work and study limitations

From the current work, it has been shown that, firstly, the ceria-coated silica nanoparticles has an improved dilatory effect on the young mouse aorta, whereas silica nanoparticles do not have a statistically significantreduced effect on dilation. The future workcan investigate

the underlying mechanisms that are responsible for the improved dilation after incubation with ceria-coated silica nanoparticles. Secondly, ceria-coated silica nanoparticles do not improve dilation in aged aortic vessels while uncoated silica nanoparticles (C3) had no detrimental effect on dilator responses. This is expected since the dilator component in aged vessels is similar to that in young vessels.

4.5.1Further characterisation of silica and ceria-coated silica nanoparticles

Additional characterisation techniques will be necessary on the silica and ceria-coated silica nanoparticles. These include:

1. Determining the concentration of oxygen vacancies using Raman spectroscopy using the calculations outlined in (Thanneeru 2004). It has been shown that ceria nanoparticles have an increased concentration of oxygen vacancies, which are responsible for their high redox potential and antioxidant properties. The Raman spectroscopy will allow the calculation of the oxygen vacancy concentration and confirm an increased concentration in the ceria-coated silica nanoparticles.

2. Establishing the oxidative capacity of silica and ceria-coated silica nanoparticles in various solutions (water, PSS and cell culture medium) using a DTT assay following the protocol outlines in (Koike and Kobayashi 2006). There are two objectives from this technique: (1) To confirm that ceria-coated silica nanoparticles have an increased antioxidant capacity when compared to silica nanoparticles and (2) that the oxidative capacities of the nanoparticles remains the same in the different suspensions (water, PSS and in cell culture medium)

4. 5.2. Nanoparticle influence on vascular function and deduction of vasodilatory mechanisms

The findings from the present study were based on limited numbers of experiments, due to the limited availability of tissue, especially that from aged mice. It will be important to confirm findings on the influence of nanoparticles on vasodilator function and the vasodilatory mechanisms that are responsible. This can be done by Increasing data from organ bath studies following the protocol outlined in this report, using young mice, to validate the current findings. For example, Silica (SilC3) nanoparticle incubation and assessment of vasodilation response (n=4 need to be conducted); Ceria-coated silica nanoparticle incubation and assessment of vasodilation response (n=3 need to be conducted).

4.5.3 Deduction of vasodilatory mechanisms in mouse aorta and the influence of nanoparticle incubation on those mechanisms

1. Establishing the vasodilatory component in mouse aorta using inhibition studies:

    a. Using L-NG-nitro-L-arginine (LNNA) to inhibit the nitric oxide (NO) pathway to assess the change in vasodilation response and effect of nanoparticle incubation

    b. Using indomethacin to inhibit the prostacyclin pathway to assess the change in vasodilation response and effect of nanoparticle incubation

    c. Using apamin and TRAM-34 to inhibit potassium channels (small conductance calcium activated and intermediate conductance calcium activated potassium channels respectively) that interfere with the endothelial derived hyperpolarising factor (EDHF) pathway

2. Establishing the mechanism of ceria-coated nanoparticle-induced altered dilation using inhibition studies by co-incubating a vasodilator inhibitor with ceria-coated nanoparticles and decipher which mechanism of vasodilation is being acted upon by the ceria-coated silica nanoparticles

4.5.4Comparison of structural features in young and old mice using histology sections

To compare the young and old mice vessel structure, histology techniques will be used including:

1. Embedding aortic vessel rings into paraffin after first fixing with paraformaldehyde and then dehydration using industrial methylated spirit and xylene. Sectioning and staining will be conducted to be able to distinguish the structural components and to look at differences
2. Embedding aortic vessel rings into OCTwhich is then frozen immediately using liquid nitrogen.Sections will then be taken and hydroethidine dye will be applied topically. Once sample was ready to be viewed, under fluorescence microscopy (Alexander, Brosnan et al. 2000)

4.5.5.Influence of silica and ceria-coated silica nanoparticles on cell viability and vasodilator function using mouse aortic endothelial cells

In order to elucidate the mechanisms behind the improved vasodilation response seen in young mice after incubation with ceria-coated silica nanoparticles, *in vitro* work will be necessary to look at vasodilatory mechanisms responsible for this effect. This includes:

1. Obtaining mouse aortic endothelial cells fromCellBiologics Inc, USA (Cat #: C57-6052) so that results are comparable to the vascular functional studies conducted on mice
2. Ensuring cells are viable by using the MTT assay, a colorimetric assay, which assesses metabolic activity of cells and therefore determines viability
3. Investigating expression of enzymes involved in the various vasodilatory pathways will be quantified using Western Blotting
4. Effect of ceria-coated silica on ROS production will be assessed using carboxy-H_2DCFDA, outlined in (Wu and Yotnda 2011). The is a fluorometric assay which can be analysed using flow cytometry, a fluorescence plate reader, or flow cytometry

5. References

Alexander, M. Y., M. J. Brosnan, C. A. Hamilton, J. P. Fennell, E. C. Beattie, E. Jardine, D. D. Heistad and A. F. Dominiczak (2000). "Gene transfer of endothelial nitric oxide synthase but not Cu/Zn superoxide dismutase restores nitric oxide availability in the SHRSP." Cardiovascular Research**47**(3): 609-617.

Alexis, F., E. M. Pridgen, R. Langer and O. C. Farokhzad (2009). Nanoparticle Technologies for Cancer Therapy. Drug Delivery. Berlin, Springer Berlin Heidelberg**:** 55-86.

Bagwe, R. P., C. Yang, L. R. Hilliard and W. Tan (2004). "Optimization of Dye-Doped Silica Nanoparticles Prepared Using a Reverse Microemulsion Method." Langmuir**20**(19): 8336-8342.

Baptista, P. V., G. Doria, P. Quaresma, M. Cavadas, C. S. Neves, I. Gomes, P. Eaton, E. Pereira and R. Franco (2011). Chapter 11 - Nanoparticles in Molecular Diagnostics. Progress in Molecular Biology and Translational Science. V. Antonio, Academic Press. **Volume 104:** 427-488.

Bartosz, M., J. Kedziora and G. Bartosz (1997). "Antioxidant and Prooxidant Properties of Captopril and Enalapril." Free Radical Biology and Medicine**23**(5): 729-735.

Bradbury, S. J., David. C.; Ford, Brian. J. (2008) "Scanning electron microscope (SEM)."

Bratic, A. and N.-G. Larsson (2013). "The role of mitochondria in aging." Journal of Clinical Investigation**123**(3): 951-957.

BSI (2011). Vocabulary - Nanoparticles.

Byrappa, K., S. Ohara and T. Adschiri (2008). "Nanoparticles synthesis using supercritical fluid technology – towards biomedical applications." Advanced Drug Delivery Reviews**60**(3): 299-327.

Chen, F., X. H. Zhang, X. D. Hu, W. Zhang, Z. C. Lou, L. H. Xie, P. D. Liu and H. Q. Zhang (2015). "Enhancement of radiotherapy by ceria nanoparticles modified with neogambogic acid in breast cancer cells." International Journal of Nanomedicine**10**: 4957-4969.

Chen, H.-I. and H.-Y. Chang (2005). "Synthesis of nanocrystalline cerium oxide particles by the precipitation method." Ceramics International**31**(6): 795-802.

Chen, J., Guo, Z., Tian, H. and Chen, X. (2016) "Production and clinical development of nanoparticles for gene delivery." Molecular Therapy: Methods & Clinical Development**(3)**: 16023

Chen, S., Y. Hou, G. Cheng, C. Zhang, S. Wang and J. Zhang (2013). "Cerium Oxide Nanoparticles Protect Endothelial Cells from Apoptosis Induced by Oxidative Stress." Biological Trace Element Research**154**(1): 156-166.

Cheng, X. and Lee, R.J. (2016) The role of helper lipids in lipid nanoparticles (LNPs) designed for oligonucleotide delivery." Advanced Drug Delivery Reviews**99**(A): 129-137

Corbierre, M. K., N. S. Cameron, M. Sutton, S. G. Mochrie, L. B. Lurio, A. Rühm and R. B. Lennox (2001). "Polymer-stabilized gold nanoparticles and their incorporation into polymer matrices." Journal of the American Chemistry Society**123**(42): 10411-10412.

Das, M., S. Patil, N. Bhargava, J.-F. Kang, L. M. Riedel, S. Seal and J. J. Hickman (2007). "Auto-catalytic ceria nanoparticles offer neuroprotection to adult rat spinal cord neurons." Biomaterials**28**(10): 1918-1925.

De Jong, A., J. Plat, A. Bast, R. W. L. Godschalk, S. Basu and R. P. Mensink (2007). "Effects of plant sterol and stanol ester consumption on lipid metabolism, antioxidant status and markers of oxidative stress, endothelial function and low-grade inflammation in patients on current statin treatment." Eur J Clin Nutr**62**(2): 263-273.

Duan, X. and Y. Li (2013). "Physicochemical Characteristics of Nanoparticles Affect Circulation, Biodistribution, Cellular Internalization, and Trafficking." Small**9**(9-10): 1521-1532.

Farooq, A., T. Mohamed, D. Whitehead and M. Azzawi (2014). "Restored Endothelial Dependent Vasodilation in Aortic Vessels after Uptake of Ceria Coated Silica Nanoparticles, *ex vivo*." Nanomedicine & Nanotechnology**5**(2).
Ford, B. J. (2008) "Transmission electron microscope."
Glass, J.J., Kent, S.J. and De Rose, R. (2016) "Enhancing dendritic cell activation and HIV vaccine effectiveness through nanoparticle vaccination." Expert Review of Vaccines**26**: 1-11
Graf, C., D. L. J. Vossen, A. Imhof and A. van Blaaderen (2003). "A General Methhod To Coat Colloidal Particles with Silica." Langmuir**19**(17): 6693-6700.
Hashem, R. M., L. A. Rashd, K. S. Hashem and H. M. Soliman (2015). "Cerium oxide nanoparticles alleviate oxidative stress and decreases Nrf-2/HO-1 in D-GALN/LPS induced hepatotoxicity." Biomedicine and Pharmacotherapy**73**: 80-86.
He, H.-W., X.-Q. Wu, W. Ren, P. Shi, X. Yao and Z.-T. Song (2012). "Synthesis of crystalline cerium dioxide hydrosol by a sol–gel method." Ceramics International**38, Supplement 1**: S501-S504.
Heckert, E. G., A. S. Karakoti, S. Seal and W. T. Self (2008). "The role of cerium redox state in the SOD mimetic activity of nanoceria." Biomaterials**29**(18): 2705-2709.
Hedrick, J. B. (2004). Rare Earths in Selected U.S. Defense Applications. 40th Forum on the Geology of Industrial Minerals, Bloomington, Indiana.
Hirst, S. M., A. Karakoti, S. Singh, W. Self, R. Tyler, S. Seal and C. M. Reilly (2013). "Bio-distribution and in vivo antioxidant effects of cerium oxide nanoparticles in mice." Environmental Toxicology**28**(2): 107-118.
Hirst, S. M., A. S. Karakoti, R. D. Tyler, N. Sriranganathan, S. Seal and C. M. Reilly (2009). "Anti-inflammatory Properties of Cerium Oxide Nanoparticles." Small**5**(24): 2848-2856.
Ibrahim, I. A., A. Zikry and M. A. Sharaf (2010). "Preparation of spherical silica nanoparticles: Stober silica." J. Am. Sci**6**(11): 985-989.
Izu, N., T. Uchida, I. Matsubara, T. Itoh, W. Shin and M. Nishibori (2011). "Formation mechanism of monodispersed spherical core–shell ceria/polymer hybrid nanoparticles." Materials Research Bulletin**46**(8): 1168-1176.
Judge, S., Y. M. Jang, A. Smith, T. Hagen and C. Leeuwenburgh (2005). "Age-associated increases in oxidative stress and antioxidant enzyme activities in cardiac interfibrillar mitochondria: implications for the mitochondrial theory of aging." The FASEB Journal**19**(3): 419-421.
Katiyar, S. K., A. Perez and H. Mukhtar (2000). "Green Tea Polyphenol Treatment to Human Skin Prevents Formation of Ultraviolet Light B-induced Pyrimidine Dimers in DNA." Clinical Cancer Research**6**(10): 3864-3869.
Kim, C. K., T. Kim, I.-Y. Choi, M. Soh, D. Kim, Y.-J. Kim, H. Jang, H.-S. Yang, J. Y. Kim, H.-K. Park, S. P. Park, S. Park, T. Yu, B.-W. Yoon, S.-H. Lee and T. Hyeon (2012). "Ceria Nanoparticles that can Protect against Ischemic Stroke." Angewandte Chemie**124**(44): 11201-11205.
Kobyliak, N. M., T. M. Falalyeyeva, O. G. Kuryk, T. V. Beregova, P. M. Bodnar, N. M. Zholobak, O. B. Shcherbakov, R. V. Bubnov and M. Spivak (2015). "Antioxidative effects of cerium dioxide nanoparticles ameliorate age-related male infertility: Optimistic results in rats and the review of clinical clues for integrative concept of men health and fertility." EPMA Journal**6**(1).
Koike, E. and T. Kobayashi (2006). "Chemical and biological oxidative effects of carbon black nanoparticles." Chemosphere**65**(6): 946-951.
Kojo, S. (2004). "Vitamin C: Basic Metabolism and It Function as an Index of Oxidative Stress." Current Medicinal Chemistry**11**(8): 1041-1064.
Kolattukudy, P. E., T. Quach, S. Bergese, S. Breckenridge, J. Hensley, R. Altschuld, G. Gordillo, S. Klenotic, C. Orosz and J. Parker-Thornburg (1998). "Myocarditis induced by

targeted expression of the MCP-1 gene in murine cardiac muscle." The American Journal of Pathology**152**(1): 101-111.
Kovacic, J. C., P. Moreno, E. G. Nabel and V. Hachinski, Valentin (2011). "Cellular Senescence, Vascular Disease, and Aging: Part 2 of a 2-Part Review: Clinical Vascular Disease in the Elderly." Circulation**123**(17): 1900-1910.
Krausz, A. E., B. L. Adler, V. Cabral, M. Navati, J. Doerner, R. A. Charafeddine, D. Chandra, H. Liang, L. Gunther, A. Clendaniel, S. Harper, J. M. Friedman, J. D. Nosanchuk and A. J. Friedman (2015). "Curcumin-encapsulated nanoparticles as innovative antimicrobial and wound healing agent." Nanomedicine: Nanotechnology, Biology and Medicine**11**(1): 195-206.
Lakatta, E. G. and D. Levy (2003). "Arterial and Cardiac Aging: Major Shareholders in Cardiovascular Disease Enterprises: Part I: Aging Arteries: A “Set Up” for Vascular Disease." Circulation**107**(1): 139-146.
Lee, J., N. Koo and D. B. Min (2004). "Reactive Oxygen Species, Aging, and Antioxidative Nutraceuticals." Comprehensive Reviews in Food Science and Food Safety**3**(1): 21-33.
Li, H., Z. Y. Yang, C. Liu, Y. P. Zeng, Y. H. Hao, Y. Gu, W. D. Wang and R. Li (2015). "PEGylated ceria nanoparticles used for radioprotection on human liver cells under γ-ray irradiation." Free Radical Biology and Medicine**87**: 26-35.
Liu, X. and Sun, J. (2010) "Endothelial cells dysfunction induced by silica nanoparticles through oxidative stress via JNK/P53 and NF-kB pathways." Biomaterials**31**: 8198-8209
Maddux, B. A., W. See, J. C. Lawrence, A. L. Goldfine, I. D. Goldfine and J. L. Evans (2001). "Protection Against Oxidative Stress—Induced Insulin Resistance in Rat L6 Muscle Cells by Micromolar Concentrations of α-Lipoic Acid." Diabetes**50**(2): 404-410.
Mandzy, N., E. Grulke and T. Druffel (2005). "Breakage of TiO2 agglomerates in electrostatically stabilized aqueous dispersions." Powder Technology**160**(2): 121-126.
Masui, T., H. Hirai, N. Imanaka, G. Adachi, T. Sakata and H. Mori (2002). "Synthesis of cerium oxide nanoparticles by hydrothermal crystallization with citric acid." Journal of Materials Science Letters**21**(6): 489-491.
McCormack, R. N., P. Mendez, S. Barkam, C. J. Neal, S. Das and S. Seal (2014). "Inhibition of Nanoceria’s Catalytic Activity due to Ce3+ Site-Specific Interaction with Phosphate Ions." The Journal of Physical Chemistry C**118**(33): 18992-19006.
Meydani, M. (2000). "Effect of functional food ingredients: vitamin E modulation of cardiovascular diseases and immune status in the elderly." The American Journal of Clinical Nutrition**71**(6): 1665s-1668s.
Muhammad, F., A. Wang, W. Qi, S. Zhang and G. Zhu (2014). "Intracellular antioxidants dissolve man-made antioxidant nanoparticles: Using redox vulnerability of nanoceria to develop a responsive drug delivery system." ACS Applied Materials and Interfaces**6**(21): 19424-19433.
NanoComposix (2012). Zeta Potential Analysis of Nanoparticles. San Diego, California, NanoComposix.
Niu, J., A. Azfer, L. M. Rogers, X. Wang and P. E. Kolattukudy (2007). "Cardioprotective effects of cerium oxide nanoparticles in a transgenic murine model of cardiomyopathy." Cardiovascular research**73**(3): 549-559.
Oh, H. and S. Kim (2007). "Synthesis of ceria nanoparticles by flame electrospray pyrolysis." Journal of Aerosol Science**38**(12): 1185-1196.
Oh, M.-H., J.-S. Lee, S. Gupta, F.-C. Chang and R. K. Singh (2010). "Preparation of monodispersed silica particles coated with ceria and control of coating thickness using sol-type precursor." Colloids and Surfaces A: Physicochemical and Engineering Aspects**355**(1–3): 1-6.
OpenStax College (2014) "Anatomy & Physiology."

Pashkow, F. J., D. G. Watumull and C. L. Campbell (2008). "Astaxanthin: A Novel Potential Treatment for Oxidative Stress and Inflammation in Cardiovascular Disease." The American Journal of Cardiology**101**(10, Supplement): S58-S68.
Patra, C. R. (2016) "Prussian blue nanoparticles and their analogues for application to cancer theranostics." Nanomedicine**11**(6): 569-572
Perez, J. M., A. Asati, S. Nath and C. Kaittanis (2008). "Synthesis of Biocompatible Dextran-Coated Nanoceria with pH-Dependent Antioxidant Properties." Small**4**(5): 552-556.
Pinna, A., L. Malfatti, G. Galleri, R. Manetti, S. Cossu, G. Rocchitta, R. Migheli, P. A. Serra and P. Innocenzi (2015). "Ceria nanoparticles for the treatment of Parkinson-like diseases induced by chronic manganese intoxication." RSC Advances**5**(26): 20432-20439.
Pryor, W. A. (2000). "Vitamin E and heart disease: Basic science to clinical intervention trials." Free Radical Biology and Medicine**28**(1): 141-164.

Radenkovic, D., Kobayashi, H., Remsey-Semmelweis, Erno., and Seifalian, A.M. (2016) "Quantum dot nanoparticle for optimization of breast cancer diagnostics and therapy in a clinical setting." Nanomedicine: Nanotechnology, Biology and Medicine**(article in press)**
Rodea-Palomares, I., K. Boltes, F. Fernández-Piñas, F. Leganés, E. García-Calvo, J. Santiago and R. Rosal (2011). "Physicochemical Characterization and Ecotoxicological Assessment of CeO2 Nanoparticles Using Two Aquatic Microorganisms." Toxicological Sciences**119**(1): 135-145.
Rzigalinski, B. A., K. Meehan, R. M. Davis, Y. Xu, W. C. Miles and C. A. Cohen (2006). "Radical nanomedicine." Nanomedicine**1**(4): 399-412.
Sathyamurthy, S., K. Leonard, J, R. T. Dabestani and M. P. Paranthaman (2005). "Reverse micellar synthesis of cerium oxide nanoparticles." Nanotechnology**16**(9): 1960.
Spiteller, G. (2001). "Lipid peroxidation in aging and age-dependent diseases." Experimental Gerontology**36**(9): 1425-1457.
Stöber, W., A. Fink and E. Bohn (1968). "Controlled growth of monodisperse silica spheres in the micron size range." Journal of Colloid and Interface Science**26**(1): 62-69.
Strobel, C., H. Oehring, R. Herrmann, M. Förster, A. Reller and I. Hilger (2015). "Fate of cerium dioxide nanoparticles in endothelial cells: exocytosis." Journal of Nanoparticle Research**17**(5): 1-14.
Tang, F., Li, L. and Chen, D. (2012) 'Mesoporous Silica Nanoparticles: Synthesis, Biocompatibility and Drug Delivery.' Advanced Materials**24** (12): 1504-1534
Thanneeru, R. J. (2004). Vacancy Engineered Doped and Undoped Nanocrystalline Rare Earth Oxide Particles for High Temperature Oxidation Resistant Coatings. Master of Science, University of Central Florida.
Tousoulis, D. (2012). "The role of nitric oxide on endothelial function." Current Vascular Pharmacology**10**(1): 4-18.
van der Loo, B., R. Labugger, J. N. Skepper, M. Bachschmid, J. Kilo, J. M. Powell, M. Palacios-Callender, J. D. Erusalimsky, T. Quaschning, T. Malinski, D. Gygi, V. Ullrich and T. F. Lüscher (2000). "Enhanced Peroxynitrite Formation Is Associated with Vascular Aging." Journal of Experimental Medicine**192**(12): 1731-1744.
Vivekananthan, D. P., M. S. Penn, S. K. Sapp, A. Hsu and E. J. Topol (2003). "Use of antioxidant vitamins for the prevention of cardiovascular disease: meta-analysis of randomised trials." The Lancet**361**(9374): 2017-2023.
Weaver, J. D. and C. L. Stabler (2015). "Antioxidant cerium oxide nanoparticle hydrogels for cellular encapsulation." Acta Biomaterialia**16**(1): 136-144.
Weseler, A. R. and A. Bast (2010). "Oxidative Stress and Vascular Function: Implications for Pharmacologic Treatments." Current Hypertension Reports**12**(3): 154-161.
Wu, D. and P. Yotnda (2011). "Production and Detection of Reactive Oxygen Species (ROS) in Cancers." Journal of Visualized Experiments : JoVE(57): 3357.

Xia, T., M. Kovochich, M. Liong, L. Mädler, B. Gilbert, H. Shi, J. I. Yeh, J. I. Zink and A. E. Nel (2008). "Comparison of the Mechanism of Toxicity of Zinc Oxide and Cerium Oxide Nanoparticles Based on Dissolution and Oxidative Stress Properties." ACS Nano**2**(10): 2121-2134.
Yang, Y.-M., A. Huang, G. Kaley and D. Sun (2009). "eNOS uncoupling and endothelial dysfunction in aged vessels." American Journal of Physiology - Heart and Circulatory Physiology**297**(5): H1829-H1836.
Yang, Z. Y., S. L. Luo, H. Li, S. W. Dong, J. He, H. Jiang, R. Li and X. C. Yang (2014). "Alendronate as a robust anchor for ceria nanoparticle surface coating: Facile binding and improved biological properties." RSC Advances**4**(104): 59965-59969.
Yatin, S. M., S. Varadarajan and D. A. Butterfield (2000). "Vitamin E Prevents Alzheimer's Amyloid ß-Peptide (1-42)-Induced Neuronal Protein Oxidation and Rective Oxygen Species Production." Journal of Alzheimer's Disease**2**(2): 123-131.
Yazici, H., E. Alpaslan and T. Webster (2015). "The Role of Dextran Coatings on the Cytotoxicity Properties of Ceria Nanoparticles Toward Bone Cancer Cells." JOM**67**(4): 804-810.
Zern, T. L., R. J. Wood, C. Greene, K. L. West, Y. Liu, D. Aggarwal, N. S. Shachter and M. L. Fernandez (2005). "Grape Polyphenols Exert a Cardioprotective Effect in Pre- and Postmenopausal Women by Lowering Plasma Lipids and Reducing Oxidative Stress." The Journal of Nutrition**135**(8): 1911-1917.

6. APPENDIX

6.1. Publications arising from the project

Tye, E., Shukur, A., Farooq, A., Wilkinson, F., Alexander, Y., Whitehead, D., and Azzawi, M. (2015) 'A comparison of silica nanoparticle uptake and their effects on young and aged murine arterial function, *ex vivo*.' *Microcirculation*, Vol.22, pp. 753-781

6.2. Chemical characterisation of nanoparticles

6.2.1. Hydrodynamic diameter

Listed below are the outputs measuring hydrodynamic diameter of various nanoparticles used in this present study. Figure 23 shows hydrodynamic diameter in silica (C3) nanoparticles and Figure 24 shows the hydrodynamic diameter of ceria-coated silica nanoparticles (SilC3Ce1).

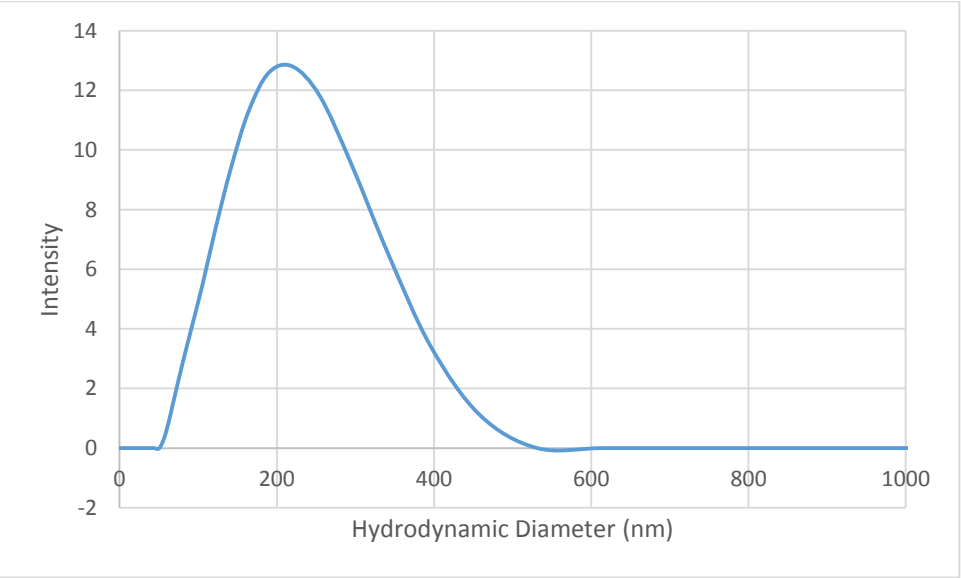

Figure 23 Hydrodynamic diameter of silica nanoparticles (SilC3) in water, as measured using DLS

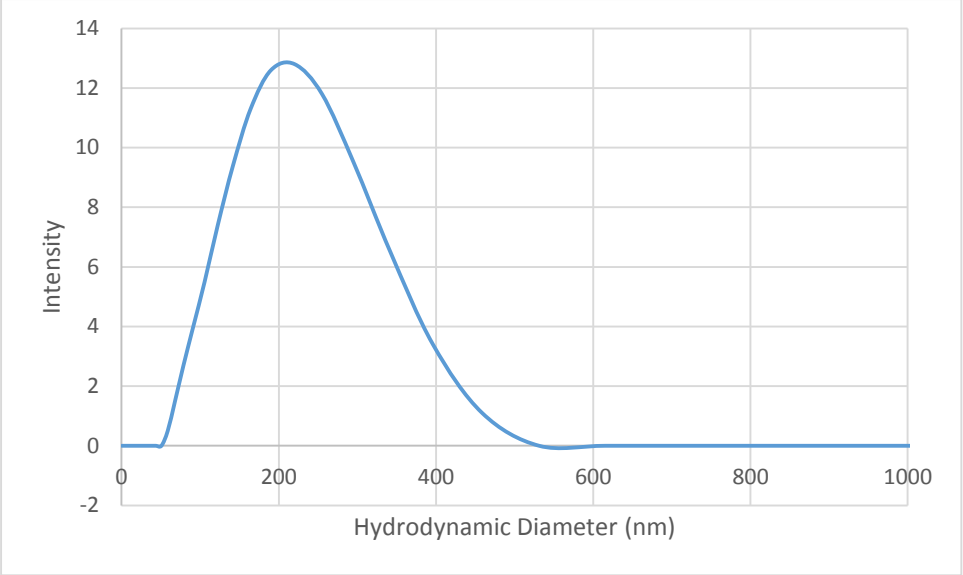

Figure 24 Hydrodynamic diameter of ceria-coated silica nanoparticles (SilC3Ce1), as measured using DLS

6.3. Calibration of organ bath system

Before each organ bath experiment was conducted, the system was calibrated by adding two 1g weights onto the transducer and adjusting the readings given on the LabChart software to read 1g and 2g when one or two weight, respectively, were added. Once these weights were removed, the reading would be at '0' and then the experiment followed as previously mentioned.

6.4 Preliminary resting tension data

Table 14 KPSS and phenylephrine response after various resting tensions were applied to the vessel

Resting Tension (g)	KPSS response achieved (g)	Phenylephrine response achieved (g)
0.05	0.010	0.02
0.10	0.035	0.1
0.20	0.045	0.00
0.30	0.015	0.00
0.40	0.040	0.00
0.50	0.025	0.00

Table 15 Acetylcholine (at 10^{-4}M and 10^{-3}M) response after various resting tensions were applied to the vessel

Resting Tension (g)	Tension achieved at Ach 10^{-4} M	Tension achieved at Ach 10^{-3} M
0.1	0.00	0.00
0.2	0.03	0.04
0.3	0.05	0.05
0.4	0.03	0.05
0.5	0.02	0.04

Based on both the KPSS, phenylephrine and acetylcholine responses, 0.4g resting tension was used for this study.

6.6. COSHH forms

Below are attached the COSHH and risk assessment forms for this study.